

## TOPICAL REVIEW

## Inverse scattering series and seismic exploration

**Arthur B Weglein<sup>1</sup>, Fernanda V Araújo<sup>2,8</sup>, Paulo M Carvalho<sup>3</sup>,  
Robert H Stolt<sup>4</sup>, Kenneth H Matson<sup>5</sup>, Richard T Coates<sup>6</sup>,  
Dennis Corrigan<sup>7,9</sup>, Douglas J Foster<sup>4</sup>, Simon A Shaw<sup>1,5</sup> and  
Haiyan Zhang<sup>1</sup>**

<sup>1</sup> University of Houston, 617 Science and Research Building 1, Houston, TX 77204, USA

<sup>2</sup> Universidade Federal da Bahia, PPPG, Brazil

<sup>3</sup> Petrobras, Avenida Chile 65 S/1402, Rio De Janeiro 20031-912, Brazil

<sup>4</sup> ConocoPhillips, PO Box 2197, Houston, TX 77252, USA

<sup>5</sup> BP, 200 Westlake Park Boulevard, Houston, TX 77079, USA

<sup>6</sup> Schlumberger Doll Research, Old Quarry Road, Ridgefield, CT 06877, USA

<sup>7</sup> ARCO, 2300 W Plano Parkway, Plano, TX 75075, USA

E-mail: aweglein@uh.edu

Received 18 February 2003

Published 9 October 2003

Online at [stacks.iop.org/IP/19/R27](http://stacks.iop.org/IP/19/R27)

### Abstract

This paper presents an overview and a detailed description of the key logic steps and mathematical-physics framework behind the development of practical algorithms for seismic exploration derived from the inverse scattering series.

There are both significant symmetries and critical subtle differences between the forward scattering series construction and the inverse scattering series processing of seismic events. These similarities and differences help explain the efficiency and effectiveness of different inversion objectives. The inverse series performs all of the tasks associated with inversion using the entire wavefield recorded on the measurement surface as input. However, certain terms in the series act as though only one specific task, and no other task, existed. When isolated, these terms constitute a task-specific subseries. We present both the rationale for seeking and methods of identifying uncoupled task-specific subseries that accomplish: (1) free-surface multiple removal; (2) internal multiple attenuation; (3) imaging primaries at depth; and (4) inverting for earth material properties.

A combination of forward series analogues and physical intuition is employed to locate those subseries. We show that the sum of the four task-specific subseries does not correspond to the original inverse series since terms with coupled tasks are never considered or computed. Isolated tasks are accomplished sequentially and, after each is achieved, the problem is restarted as though that isolated task had never existed. This strategy avoids choosing portions of the series, at any stage, that correspond to a combination of tasks, i.e.,

<sup>8</sup> Present address: ExxonMobil Upstream Research Company, PO Box 2189, Houston, TX 77252, USA.

<sup>9</sup> Present address: 5821 SE Madison Street, Portland, OR 97215, USA.

no terms corresponding to coupled tasks are ever computed. This inversion in stages provides a tremendous practical advantage. The achievement of a task is a form of useful information exploited in the redefined and restarted problem; and the latter represents a critically important step in the logic and overall strategy. The individual subseries are analysed and their strengths, limitations and prerequisites exemplified with analytic, numerical and field data examples.

(Some figures in this article are in colour only in the electronic version)

## 1. Introduction and background

In exploration seismology, a man-made source of energy on or near the surface of the earth generates a wave that propagates into the subsurface. When the wave reaches a reflector, i.e., a location of a rapid change in earth material properties, a portion of the wave is reflected upward towards the surface. In marine exploration, the reflected waves are recorded at numerous receivers (hydrophones) along a towed streamer in the water column just below the air–water boundary (see figure 1).

The objective of seismic exploration is to determine subsurface earth properties from the recorded wavefield in order to locate and delineate subsurface targets by estimating the type and extent of rock and fluid properties for their hydrocarbon potential.

The current need for more effective and reliable techniques for extracting information from seismic data is driven by several factors including (1) the higher acquisition and drilling cost, the risk associated with the industry trend to explore and produce in deeper water and (2) the serious technical challenges associated with deep water, in general, and specifically with imaging beneath a complex and often ill-defined overburden.

An event is a distinct arrival of seismic energy. Seismic reflection events are catalogued as primary or multiple depending on whether the energy arriving at the receiver has experienced one or more upward reflections, respectively (see figure 2). In seismic exploration, multiply reflected events are called multiples and are classified by the location of the downward reflection between two upward reflections. Multiples that have experienced at least one downward reflection at the air–water or air–land surface (free surface) are called free-surface multiples. Multiples that have all of their downward reflections below the free surface are called internal multiples. Methods for extracting subsurface information from seismic data typically assume that the data consist exclusively of primaries. The latter model then allows one upward reflection process to be associated with each recorded event. The primaries-only assumption simplifies the processing of seismic data for determining the spatial location of reflectors and the local change in earth material properties across a reflector. Hence, to satisfy this assumption, multiple removal is a requisite to seismic processing. Multiple removal is a long-standing problem and while significant progress has been achieved over the past decade, conceptual and practical challenges remain. The inability to remove multiples can lead to multiples masquerading or interfering with primaries causing false or misleading interpretations and, ultimately, poor drilling decisions. The primaries-only assumption in seismic data analysis is shared with other fields of inversion and non-destructive evaluation, e.g., medical imaging and environmental hazard surveying using seismic probes or ground penetrating radar. In these fields, the common violation of these same assumptions can lead to erroneous medical diagnoses and hazard detection with unfortunate and injurious human and environmental

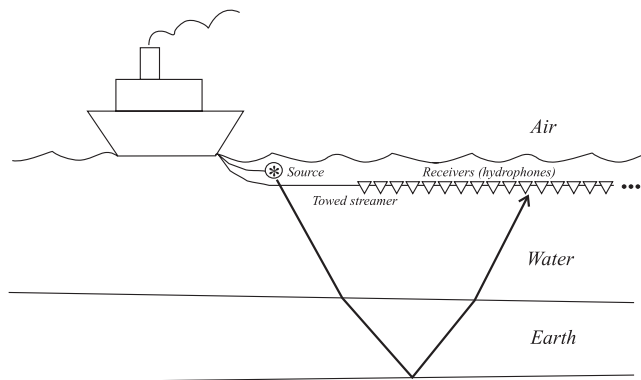


**Figure 1.** Marine seismic exploration geometry: \* and  $\nabla$  indicate the source and receiver, respectively. The boat moves through the water towing the source and receiver arrays and the experiment is repeated at a multitude of surface locations. The collection of the different source–receiver wavefield measurements defines the seismic reflection data.

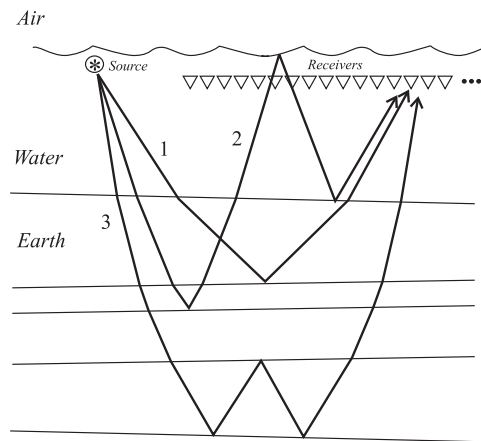


**Figure 2.** Marine primaries and multiples: 1, 2 and 3 are examples of primaries, free-surface multiples and internal multiples, respectively.

consequences. In addition, all these diverse fields typically assume that a single weak scattering model is adequate to generate the reflection data.

Even when multiples are removed from seismic reflection data, the challenges for accurate imaging (locating) and inversion across reflectors are serious, especially when the medium of propagation is difficult to adequately define, the geometry of the target is complex and the contrast in earth material properties is large. The latter large contrast property condition is by itself enough to cause linear inverse methods to collide with their assumptions.

The location and delineation of hydrocarbon targets beneath salt, basalt, volcanics and karsted sediments are of high economic importance in the petroleum industry today. For these complex geological environments, the common requirement of all current methods for the imaging-inversion of primaries for an accurate (or at least adequate) model of the medium above the target is often not achievable in practice, leading to erroneous, ambivalent or misleading predictions. These difficult imaging conditions often occur in the deep water Gulf of Mexico, where the confluence of large hydrocarbon reserves beneath salt and the high cost of drilling

(and, hence, lower tolerance for error) in water deeper than 1 km drives the demand for much more effective and reliable seismic data processing methods.

In this topical review, we will describe how the inverse scattering series has provided the promise of an entire new vision and level of seismic capability and effectiveness. That promise has already been realized for the removal of free-surface and internal multiples. We will also describe the recent research progress and results on the inverse series for the processing of primaries. Our objectives in writing this topical review are:

- (1) to provide both an overview and a more comprehensive mathematical-physics description of the new inverse-scattering-series-based seismic processing concepts and practical industrial production strength algorithms;
- (2) to describe and exemplify the strengths and limitations of these seismic processing algorithms and to discuss open issues and challenges; and
- (3) to explain how this work exemplifies a general philosophy for and approach (strategy and tactics) to defining, prioritizing, choosing and then solving significant real-world problems from developing new fundamental theory, to analysing issues of limitations of field data, to satisfying practical prerequisites and computational requirements.

The problem of determining earth material properties from seismic reflection data is an inverse scattering problem and, specifically, a non-linear inverse scattering problem. Although an overview of all seismic methods is well beyond the scope of this review, it is accurate to say that prior to the early 1990s, all deterministic methods used in practice in exploration seismology could be viewed as different realizations of a linear approximation to inverse scattering, the inverse Born approximation [1–3]. Non-linear inverse scattering series methods were first introduced and adapted to exploration seismology in the early 1980s [4] and practical algorithms first demonstrated in 1997 [5].

All scientific methods assume a model that starts with statements and assumptions that indicate the inclusion of some (and ignoring of other) phenomena and components of reality. Earth models used in seismic exploration include acoustic, elastic, homogeneous, heterogeneous, anisotropic and anelastic; the assumed dimension of change in subsurface material properties can be 1D, 2D or 3D; the geometry of reflectors can be, e.g., planar, corrugated or diffractive; and the man-made source and the resultant incident field must be described as well as both the character and distribution of the receivers.

Although 2D and 3D closed form complete integral equation solutions exist for the Schrödinger equation (see [6]), there is no analogous closed form complete multi-dimensional inverse solution for the acoustic or elastic wave equations. The push to develop complete multi-dimensional non-linear seismic inversion methods came from: (1) the need to remove multiples in a complex multi-dimensional earth and (2) the interest in a more realistic model for primaries. There are two different origins and forms of non-linearity in the description and processing of seismic data. The first derives from the intrinsic non-linear relationship between certain physical quantities. Two examples of this type of non-linearity are:

- (1) multiples and reflection coefficients of the reflectors that serve as the source of the multiply reflected events and
- (2) the intrinsic non-linear relationship between the angle-dependent reflection coefficient at any reflector and the changes in elastic property changes.

The second form of non-linearity originates from forward and inverse descriptions that are, e.g., in terms of estimated rather than actual propagation experiences. The latter non-linearity has the sense of a Taylor series. Sometimes a description consists of a combination of these

two types of non-linearity as, e.g., occurs in the description and removal of internal multiples in the forward and inverse series, respectively.

The absence of a closed form exact inverse solution for a 2D (or 3D) acoustic or elastic earth caused us to focus our attention on non-closed or series forms as the only candidates for direct multi-dimensional exact seismic processing. An inverse series can be written, at least formally, for any differential equation expressed in a perturbative form.

This article describes and illustrates the development of concepts and practical methods from the inverse scattering series for multiple attenuation and provides promising conceptual and algorithmic results for primaries. Fifteen years ago, the processing of primaries was conceptually more advanced and effective in comparison to the methods for removing multiples. Now that situation is reversed. At that earlier time, multiple removal methods assumed a 1D earth and knowledge of the velocity model, whereas the processing of primaries allowed for a multi-dimensional earth and also required knowledge of the 2D (or 3D) velocity model for imaging and inversion. With the introduction of the inverse scattering series for the removal of multiples during the past 15 years, the processing of multiples is now conceptually more advanced than the processing of primaries since, with a few exceptions (e.g., migration-inversion and reverse time migration) the processing of primaries have remained relatively stagnant over that same 15 year period. Today, all free-surface and internal multiples can be attenuated from a multi-dimensional heterogeneous earth with absolutely no knowledge of the subsurface whatsoever before or after the multiples are removed. On the other hand, imaging and inversion of primaries at depth remain today where they were 15 years ago, requiring, e.g., an adequate velocity for an adequate image. The inverse scattering subseries for removing free surface and internal multiples provided the first comprehensive theory for removing all multiples from an arbitrary heterogeneous earth without any subsurface information whatsoever. Furthermore, taken as a whole, the inverse series provides a fully inclusive theory for processing both primaries and multiples directly in terms of an inadequate velocity model, without updating or in any other way determining the accurate velocity configuration. Hence, the inverse series and, more specifically, its subseries that perform imaging and inversion of primaries have the potential to allow processing primaries to catch up with processing multiples in concept and effectiveness.

## 2. Seismic data and scattering theory

### 2.1. *The scattering equation*

Scattering theory is a form of perturbation analysis. In broad terms, it describes how a perturbation in the properties of a medium relates a perturbation to a wavefield that experiences that perturbed medium. It is customary to consider the original unperturbed medium as the reference medium. The difference between the actual and reference media is characterized by the perturbation operator. The corresponding difference between the actual and reference wavefields is called the scattered wavefield. Forward scattering takes as input the reference medium, the reference wavefield and the perturbation operator and outputs the actual wavefield. Inverse scattering takes as input the reference medium, the reference wavefield and values of the actual field on the measurement surface and outputs the difference between actual and reference medium properties through the perturbation operator. Inverse scattering theory methods typically assume the support of the perturbation to be on one side of the measurement surface. In seismic application, this condition translates to a requirement that the difference between actual and reference media be non-zero only below the source–receiver surface. Consequently, in seismic applications, inverse scattering methods require that the reference medium agrees with the actual at and above the measurement surface.

For the marine seismic application, the sources and receivers are located within the water column and the simplest reference medium is a half-space of water bounded by a free surface at the air–water interface. Since scattering theory relates the difference between actual and reference wavefields to the difference between their medium properties, it is reasonable that the mathematical description begin with the differential equations governing wave propagation in these media. Let

$$\mathbf{L}G = -\delta(\mathbf{r} - \mathbf{r}_s) \quad (1)$$

and

$$\mathbf{L}_0G_0 = -\delta(\mathbf{r} - \mathbf{r}_s) \quad (2)$$

where  $\mathbf{L}$ ,  $\mathbf{L}_0$  and  $G$ ,  $G_0$  are the actual and reference differential operators and Green functions, respectively, for a single temporal frequency,  $\omega$ , and  $\delta(\mathbf{r} - \mathbf{r}_s)$  is the Dirac delta function.  $\mathbf{r}$  and  $\mathbf{r}_s$  are the field point and source location, respectively. Equations (1) and (2) assume that the source and receiver signatures have been deconvolved. The impulsive source is ignited at  $t = 0$ .  $G$  and  $G_0$  are the matrix elements of the Green operators,  $\mathbf{G}$  and  $\mathbf{G}_0$ , in the spatial coordinates and temporal frequency representation.  $\mathbf{G}$  and  $\mathbf{G}_0$  satisfy  $\mathbf{L}\mathbf{G} = -\mathbb{I}$  and  $\mathbf{L}_0\mathbf{G}_0 = -\mathbb{I}$ , where  $\mathbb{I}$  is the unit operator. The perturbation operator,  $\mathbf{V}$ , and the scattered field operator,  $\mathbf{\Psi}_s$ , are defined as follows:

$$\mathbf{V} \equiv \mathbf{L} - \mathbf{L}_0, \quad (3)$$

$$\mathbf{\Psi}_s \equiv \mathbf{G} - \mathbf{G}_0. \quad (4)$$

$\mathbf{\Psi}_s$  is not itself a Green operator. The Lippmann–Schwinger equation is the fundamental equation of scattering theory. It is an operator identity that relates  $\mathbf{\Psi}_s$ ,  $\mathbf{G}_0$ ,  $\mathbf{V}$  and  $\mathbf{G}$  [7]:

$$\mathbf{\Psi}_s = \mathbf{G} - \mathbf{G}_0 = \mathbf{G}_0\mathbf{V}\mathbf{G}. \quad (5)$$

In the coordinate representation, (5) is valid for all positions of  $\mathbf{r}$  and  $\mathbf{r}_s$  whether or not they are outside the support of  $\mathbf{V}$ . A simple example of  $\mathbf{L}$ ,  $\mathbf{L}_0$  and  $\mathbf{V}$  when  $\mathbf{G}$  corresponds to a pressure field in an inhomogeneous acoustic medium [8] is

$$\mathbf{L} = \frac{\omega^2}{K} + \nabla \cdot \left( \frac{1}{\rho} \nabla \right),$$

$$\mathbf{L}_0 = \frac{\omega^2}{K_0} + \nabla \cdot \left( \frac{1}{\rho_0} \nabla \right)$$

and

$$\mathbf{V} = \omega^2 \left( \frac{1}{K} - \frac{1}{K_0} \right) + \nabla \cdot \left[ \left( \frac{1}{\rho} - \frac{1}{\rho_0} \right) \nabla \right], \quad (6)$$

where  $K$ ,  $K_0$ ,  $\rho$  and  $\rho_0$  are the actual and reference bulk moduli and densities, respectively. Other forms that are appropriate for elastic isotropic media and a homogeneous reference begin with the generalization of (1), (2) and (5) where matrix operators

$$\mathbf{G} = \begin{pmatrix} G^{PP} & G^{PS} \\ G^{SP} & G^{SS} \end{pmatrix}$$

and

$$\mathbf{G}_0 = \begin{pmatrix} G_0^P & 0 \\ 0 & G_0^S \end{pmatrix}$$

express the increased channels available for propagation and scattering and

$$\mathbf{V} = \begin{pmatrix} V^{PP} & V^{PS} \\ V^{SP} & V^{SS} \end{pmatrix}$$

is the perturbation operator in an elastic world [3, 9].

## 2.2. Forward and inverse series in operator form

To derive the forward scattering series, (5) can be expanded in an infinite series through a substitution of higher order approximations for  $\mathbf{G}$  (starting with  $\mathbf{G}_0$ ) in the right-hand member of (5) yielding

$$\Psi_s \equiv \mathbf{G} - \mathbf{G}_0 = \mathbf{G}_0 \mathbf{V} \mathbf{G}_0 + \mathbf{G}_0 \mathbf{V} \mathbf{G}_0 \mathbf{V} \mathbf{G}_0 + \dots \quad (7)$$

and providing  $\Psi_s$  in orders of the perturbation operator,  $\mathbf{V}$ . Equation (7) can be rewritten as

$$\Psi_s = (\Psi_s)_1 + (\Psi_s)_2 + (\Psi_s)_3 + \dots \quad (8)$$

where  $(\Psi_s)_n \equiv \mathbf{G}_0 (\mathbf{V} \mathbf{G}_0)^n$  is the portion of  $\Psi_s$  that is  $n$ th order in  $\mathbf{V}$ . The inverse series of (7) is an expansion for  $\mathbf{V}$  in orders (or powers) of the measured values of  $\Psi_s \equiv (\Psi_s)_m$ . The measured values of  $\Psi_s = (\Psi_s)_m$  constitute the data,  $D$ . Expand  $\mathbf{V}$  as a series

$$\mathbf{V} = \mathbf{V}_1 + \mathbf{V}_2 + \mathbf{V}_3 + \dots \quad (9)$$

where  $\mathbf{V}_n$  is the portion of  $\mathbf{V}$  that is  $n$ th order in the data,  $D$ .

To find  $\mathbf{V}_1, \mathbf{V}_2, \mathbf{V}_3, \dots$  and, hence,  $\mathbf{V}$ , first substitute the inverse form (9) into the forward (7)

$$\begin{aligned} \Psi_s = \mathbf{G}_0 (\mathbf{V}_1 + \mathbf{V}_2 + \dots) \mathbf{G}_0 + \mathbf{G}_0 (\mathbf{V}_1 + \mathbf{V}_2 + \dots) \mathbf{G}_0 (\mathbf{V}_1 + \mathbf{V}_2 + \dots) \mathbf{G}_0 \\ + \mathbf{G}_0 (\mathbf{V}_1 + \mathbf{V}_2 + \dots) \mathbf{G}_0 (\mathbf{V}_1 + \mathbf{V}_2 + \dots) \mathbf{G}_0 (\mathbf{V}_1 + \mathbf{V}_2 + \dots) \mathbf{G}_0 + \dots \end{aligned} \quad (10)$$

Evaluate both sides of (10) on the measurement surface and set terms of equal order in the data equal. The first order terms are

$$(\Psi_s)_m = D = (\mathbf{G}_0 \mathbf{V}_1 \mathbf{G}_0)_m, \quad (11)$$

where  $(\Psi_s)_m$  are the measured values of the scattered field  $\Psi_s$ . The second order terms are

$$0 = (\mathbf{G}_0 \mathbf{V}_2 \mathbf{G}_0)_m + (\mathbf{G}_0 \mathbf{V}_1 \mathbf{G}_0 \mathbf{V}_1 \mathbf{G}_0)_m, \quad (12)$$

the third order terms are

$$0 = (\mathbf{G}_0 \mathbf{V}_3 \mathbf{G}_0)_m + (\mathbf{G}_0 \mathbf{V}_1 \mathbf{G}_0 \mathbf{V}_2 \mathbf{G}_0)_m + (\mathbf{G}_0 \mathbf{V}_2 \mathbf{G}_0 \mathbf{V}_1 \mathbf{G}_0)_m + (\mathbf{G}_0 \mathbf{V}_1 \mathbf{G}_0 \mathbf{V}_1 \mathbf{G}_0 \mathbf{V}_1 \mathbf{G}_0)_m \quad (13)$$

and the  $n$ th order terms are

$$0 = (\mathbf{G}_0 \mathbf{V}_n \mathbf{G}_0)_m + (\mathbf{G}_0 \mathbf{V}_1 \mathbf{G}_0 \mathbf{V}_{n-1} \mathbf{G}_0)_m + \dots + (\mathbf{G}_0 \mathbf{V}_1 \mathbf{G}_0 \mathbf{V}_1 \mathbf{G}_0 \mathbf{V}_1 \dots \mathbf{G}_0 \mathbf{V}_1 \mathbf{G}_0)_m. \quad (14)$$

To solve these equations, start with (11) and invert the  $\mathbf{G}_0$  operators on both sides of  $\mathbf{V}_1$ . Then substitute  $\mathbf{V}_1$  into (12) and perform the same inversion operation as in (11) to invert the  $\mathbf{G}_0$  operators that sandwich  $\mathbf{V}_2$ . Now substitute  $\mathbf{V}_1$  and  $\mathbf{V}_2$ , found from (11) and (12), into (13) and again invert the  $\mathbf{G}_0$  operators that bracket  $\mathbf{V}_3$  and in this manner continue to compute any  $\mathbf{V}_n$ . This method for determining  $\mathbf{V}_1, \mathbf{V}_2, \mathbf{V}_3, \dots$  and hence  $\mathbf{V} = \sum_{n=1}^{\infty} \mathbf{V}_n$  is an explicit direct inversion formalism that, in principle, can accommodate a wide variety of physical phenomena and concomitant differential equations, including multi-dimensional acoustic, elastic and certain forms of anelastic wave propagation. Because a closed or integral equation solution is currently not available for the multi-dimensional forms of the latter equations and a multi-dimensional earth model is the minimum requirement for developing relevant and differential technology, the inverse scattering series is the new focus of attention for those seeking significant heightened realism, completeness and effectiveness beyond linear and/or 1D and/or small contrast techniques.

In the derivation of the inverse series equations (11)–(14) there is no assumption about the closeness of  $\mathbf{G}_0$  to  $\mathbf{G}$ , nor of the closeness of  $\mathbf{V}_1$  to  $\mathbf{V}$ , nor are  $\mathbf{V}$  or  $\mathbf{V}_1$  assumed to be small in any sense. Equation (11) is an exact equation for  $\mathbf{V}_1$ . All that is assumed is that  $\mathbf{V}_1$  is the portion of  $\mathbf{V}$  that is linear in the data.

If one were to assume that  $\mathbf{V}_1$  is close to  $\mathbf{V}$  and then treat (11) as an approximate solution for  $\mathbf{V}$ , that would then correspond to the inverse Born approximation. In the formalism of the inverse scattering series, the assumption of  $\mathbf{V} \approx \mathbf{V}_1$  is never made. The inverse Born approximation inputs the data  $D$  and  $\mathbf{G}_0$  and outputs  $\mathbf{V}_1$  which is then treated as an approximate  $\mathbf{V}$ . The forward Born approximation assumes that, in some sense,  $\mathbf{V}$  is small and the inverse Born assumes that the data,  $(\Psi_s)_m$ , are small. The forward and inverse Born approximations are two separate and distinct methods with different inputs and objectives. The forward Born approximation for the scattered field,  $\Psi_s$ , uses a linear truncation of (7) to estimate  $\Psi_s$ :

$$\Psi_s \cong \mathbf{G}_0 \mathbf{V} \mathbf{G}_0$$

and inputs  $\mathbf{G}_0$  and  $\mathbf{V}$  to find an approximation to  $\Psi_s$ . The inverse Born approximation inputs  $D$  and  $\mathbf{G}_0$  and solves for  $\mathbf{V}_1$  as the approximation to  $\mathbf{V}$  by inverting

$$(\Psi_s)_m = D \cong (\mathbf{G}_0 \mathbf{V} \mathbf{G}_0)_m.$$

All of current seismic processing methods for imaging and inversion are different incarnations of using (11) to find an approximation for  $\mathbf{V}$  [3], where  $G_0 \approx G$ , and that fact explains the continuous and serious effort in seismic and other applications to build ever more realism and completeness into the reference differential operator,  $\mathbf{L}_0$ , and its impulse response,  $\mathbf{G}_0$ . As with all technical approaches, the latter road (and current mainstream seismic thinking) eventually leads to a stage of maturity where further allocation of research and technical resource will no longer bring commensurate added value or benefit. The inverse series methods provide an opportunity to achieve objectives in a direct and purposeful manner well beyond the reach of linear methods for any given level of *a priori* information.

### 2.3. The inverse series is not iterative linear inversion

The inverse scattering series is a procedure that is separate and distinct from iterative linear inversion. Iterative linear inversion starts with (11) and solves for  $\mathbf{V}_1$ . Then a new reference operator,  $\mathbf{L}'_0 = \mathbf{L}_0 + \mathbf{V}_1$ , impulse response,  $G'_0$  (where  $\mathbf{L}'_0 G'_0 = -\delta$ ), and data,  $D' = (G - G'_0)_m$ , are input to a new linear inverse form

$$D' = (\mathbf{G}'_0 \mathbf{V}'_1 \mathbf{G}'_0)_m$$

where a new operator,  $\mathbf{G}'_0$ , has to then be inverted from both sides of  $\mathbf{V}'_1$ . These linear steps are iterated and at each step a new, and in general more complicated, operator (or matrix, Fréchet derivative or sensitivity matrix) must be inverted. In contrast, the inverse scattering series equations (11)–(14) invert the same original input operator,  $\mathbf{G}_0$ , at each step.

### 2.4. Development of the inverse series for seismic processing

The inverse scattering series methods were first developed by Moses [10], Prosser [11] and Razavy [12] and were transformed for application to a multi-dimensional earth and exploration seismic reflection data by Weglein *et al* [4] and Stolt and Jacobs [13]. The first question in considering a series solution is the issue of convergence followed closely by the question of rate of convergence. The important pioneering work on convergence criteria for the inverse series by Prosser [11] provides a condition which is difficult to translate into a statement on the size and duration of the contrast between actual and reference media. Faced with that lack of theoretical guidance, empirical tests of the inverse series were performed by Carvalho [14] for a 1D acoustic medium. Test results indicated that starting with no *a priori* information, convergence was observed but appeared to be restricted to small contrasts and duration of the perturbation. Convergence was only observed when the difference between actual earth



acoustic velocity and water (reference) velocity was less than approximately 11%. Since, for marine exploration, the acoustic wave speed in the earth is generally larger than 11% of the acoustic wave speed in water ( $1500 \text{ m s}^{-1}$ ), the practical value of the entire series without *a priori* information appeared to be quite limited.

A reasonable response might seem to be to use seismic methods that estimate the velocity trend of the earth to try to get the reference medium proximal to the actual and that in turn could allow the series to possibly converge. The problem with that line of reasoning was that velocity trend estimation methods assumed that multiples were removed prior to that analysis. Furthermore, concurrent with these technical deliberations and strategic decisions (around 1989–90) was the unmistakably consistent and clear message heard from petroleum industry operating units that inadequate multiple removal was an increasingly prioritized and serious impediment to their success.

Methods for removing multiples at that time assumed either one or more of the following: (1) the earth was 1D, (2) the velocity model was known, (3) the reflectors generating the multiples could be defined, (4) different patterns could be identified in waves from primaries and multiples or (5) primaries were random and multiples were periodic. All of these assumptions were seriously violated in deep water and/or complex geology and the methods based upon them often failed to perform, or produced erroneous or misleading results.

The interest in multiples at that time was driven in large part by the oil industry trend to explore in deep water ( $>1 \text{ km}$ ) where the depth alone can cause multiple removal methods based on periodicity to seriously violate their assumptions. Targets associated with complex multi-dimensional heterogeneous and difficult to estimate geologic conditions presented challenges for multiple removal methods that rely on having 1D assumptions or knowledge of inaccessible details about the reflectors that were the source of these multiples.

The inverse scattering series is the only multi-dimensional direct inversion formalism that can accommodate arbitrary heterogeneity directly in terms of the reference medium, through  $\mathbf{G}_0$ , i.e., with estimated rather than actual propagation,  $\mathbf{G}$ . The confluence of these factors led to the development of thinking that viewed inversion as a series of tasks or stages and to viewing multiple removal as a step within an inversion machine which could perhaps be identified, isolated and examined for its convergence properties and demands on *a priori* information and data.

### 2.5. Subseries of the inverse series

A combination of factors led to imagining inversion in terms of steps or stages with intermediate objectives towards the ultimate goal of identifying earth material properties. These factors are:

- (1) the inverse series represents the only multi-dimensional direct seismic inversion method that performs its mathematical operations directly in terms of a single, fixed, unchanging and assumed to be inadequate  $\mathbf{G}_0$ , i.e., which is assumed not to be equal to the adequate propagator,  $\mathbf{G}$ ;
- (2) numerical tests that suggested an apparent lack of robust convergence of the overall series (when starting with no *a priori* information);
- (3) seismic methods that are used to determine *a priori* reference medium information, e.g., reference propagation velocity, assume the data consist of primaries and hence were (and are) impeded by the presence of multiples;
- (4) the interest in extracting something of value from the only formalism for complete direct multi-dimensional inversion; and
- (5) the clear and unmitigable industry need for more effective methods that remove multiples especially in deep water and/or from data collected over an unknown, complex, ill-defined and heterogeneous earth.

Each stage in inversion was defined as achieving a task or objective: (1) removing free-surface multiples; (2) removing internal multiples; (3) locating and imaging reflectors in space; and (4) determining the changes in earth material properties across those reflectors. The idea was to identify, within the overall series, specific distinct subseries that performed these focused tasks and to evaluate these subseries for convergence, requirements for *a priori* information, rate of convergence, data requirements and theoretical and practical prerequisites. It was imagined (and hoped) that perhaps a subseries for one specific task would have a more favourable attitude towards, e.g., convergence in comparison to the entire series. These tasks, if achievable, would bring practical benefit on their own and, since they are contained within the construction of  $\mathbf{V}_1, \mathbf{V}_2, \dots$  in (12)–(14), each task would be realized from the inverse scattering series directly in terms of the data,  $D$ , and reference wave propagation,  $\mathbf{G}_0$ .

At the outset, many important issues regarding this new task separation strategy were open (and some remain open). Among them were

- (1) Does the series in fact uncouple in terms of tasks?
- (2) If it does uncouple, then how do you identify those uncoupled task-specific subseries?
- (3) Does the inverse series view multiples as noise to be removed, or as signal to be used for helping to image/invert the target?
- (4) Do the subseries derived for individual tasks require different algorithms for different earth model types (e.g., acoustic version and elastic version)?
- (5) How can you know or determine, in a given application, how many terms in a subseries will be required to achieve a certain degree of effectiveness?

We will address and respond to these questions in this article and list others that are outstanding or the subject of current investigation.

How do you identify a task-specific subseries? The pursuit of task-specific subseries used several different types of analysis with testing of new concepts to evaluate, refine and develop embryonic thinking largely based on analogues and physical intuition. To begin, the forward and inverse series, (7) and (11)–(14), have a tremendous symmetry. The forward series produces the scattered wavefield,  $\Psi_s$ , from a sum of terms each of which is composed of the operator,  $\mathbf{G}_0$ , acting on  $\mathbf{V}$ . When evaluated on the measurement surface, the forward series creates all of the data,  $(\Psi_s)_m = D$ , and contains all recorded primaries and multiples. The inverse series produces  $\mathbf{V}$  from a series of terms each of which can be interpreted as the operator  $\mathbf{G}_0$  acting on the recorded data,  $D$ . Hence, in scattering theory the same operator  $\mathbf{G}_0$  as acts on  $\mathbf{V}$  to create data acts on  $D$  to invert data. If we consider

$$(\mathbf{G}_0 \mathbf{V} \mathbf{G}_0)_m = (\mathbf{G}_0 (\mathbf{V}_1 + \mathbf{V}_2 + \mathbf{V}_3 + \dots) \mathbf{G}_0)_m$$

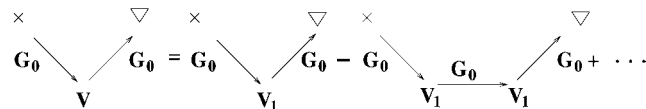
and use (12)–(14), we find

$$(\mathbf{G}_0 \mathbf{V} \mathbf{G}_0)_m = (\mathbf{G}_0 \mathbf{V}_1 \mathbf{G}_0)_m - (\mathbf{G}_0 \mathbf{V}_1 \mathbf{G}_0 \mathbf{V}_1 \mathbf{G}_0)_m + \dots \quad (15)$$

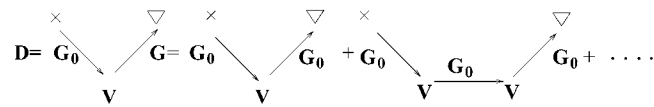
There is a remarkable symmetry between the inverse series (15) and the forward series (7) evaluated on the measurement surface:

$$(\Psi_s)_m = (\mathbf{G}_0 \mathbf{V} \mathbf{G}_0)_m + (\mathbf{G}_0 \mathbf{V} \mathbf{G}_0 \mathbf{V} \mathbf{G}_0)_m + \dots \quad (16)$$

In terms of diagrams, the inverse series for  $\mathbf{V}$ , (15) can be represented as



(the symbols  $\times$  and  $\nabla$  indicate a source and receiver, respectively) while the forward series for the data,  $(\Psi_s)_m \equiv D$ , can be represented as



This diagrammatic comparison represents opportunities for relating forward and inverse processes.

The forward and inverse problems are not ‘inverses’ of each other in a formal sense—meaning that the forward creates data but the inverse does not annihilate data: it inverts data. Nevertheless, the inverse scattering task-specific subseries while inputting all the data,  $D$  (in common with all terms in the inverse series), were thought to carry out certain actions, functions or tasks on specific subsets of the data, e.g., free-surface multiples, internal multiples and primaries. Hence, we postulated that if we could work out how those events were created in the forward series in terms of  $G_0$  and  $V$ , perhaps we could work out how those events were processed in the inverse series when once again  $G_0$  was acting on  $D$ . That intuitive leap was later provided a somewhat rigorous basis for free-surface multiples. The more challenging internal multiple attenuation subseries and the distinct subseries that image and invert primaries at depth without the velocity model while having attracted some welcome and insightful mathematical-physics rigour [15] remain with certain key steps in their logic based on plausibility, empirical tests and physical intuition.

In [5], the objective and measure of efficacy is how well the identified internal multiple attenuation algorithm removes or eliminates actual internal multiples. That is a difficult statement to make precise and rigorous since both the creation (description) and removal require an infinite number of terms in the forward and inverse series, respectively. The first term in the series that removes internal multiples of a given order is identified as the internal multiple attenuator (of that order) and is tested with actual analytic, numerical and field data to determine and define (within the analytic example) precise levels of effectiveness. A sampling of those exercises is provided in the section on multiple attenuation examples. In contrast, ten Kroode [15] defines the internal multiple attenuation problem somewhat differently: how well does the inverse scattering internal multiple attenuator remove an approximate internal multiple represented by the first term in an internal multiple forward series. The latter is a significantly different problem statement and objective from that of Weglein *et al* [5] but one that lends itself to mathematical analysis. We would argue that the former problem statement presented by Weglein *et al* [5], while much more difficult to define from a compact mathematical analysis point of view, has merit in that it judges its effectiveness by a standard that corresponds to the actual problem that needs to be addressed: the removal of internal multiples. In fact, judging the efficacy of the internal multiple attenuator by how well it removes the ‘Born approximation’ to internal multiples rolls the more serious error of travel time prediction in the latter forward model into the removal analysis with a resulting discounting of the actual power of the internal multiple attenuator in removing actual internal multiples. The leading order term in the removal series, that corresponds to the inverse scattering attenuation algorithm, has significantly greater effectiveness and more robust performance on actual internal multiples than on the Born approximation to those multiples. As the analytic example in the later section demonstrates, the inverse scattering attenuator precisely predicts the time for all internal multiples and approximates well the amplitude for P–P data, without any need whatsoever for estimating the velocity of the medium. The forward Born approximation to internal multiple data will have timing errors in comparison with actual internal multiples; hence analysing and testing the attenuator on those approximate data brings in issues due to the approximation of

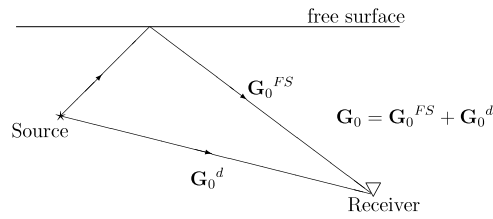


**Figure 3.** The marine configuration and reference Green function.

the forward data in the test that are misattributed to the properties of the attenuator. Tests such as those presented in [16, 17] and in the latter sections of this article are both more realistic and positive for the properties of the attenuator when tested and evaluated on real, in contrast to approximate, internal multiples.

In fact, for internal multiples, understanding how the forward scattering series produces an event only hints at where the inverse process might be located. That ‘hint’, due to a symmetry between event creation and event processing for inversion, turned out to be a suggestion, with an infinite number of possible realizations. Intuition, testing and subtle refinement of concepts ultimately pointed to where the inverse process was located. Once the location was identified, further rationalizations could be provided, in hindsight, to explain the choice among the plethora of possibilities. Intuition has played an important role in this work, which is neither an apology nor an expression of hubris, but a normal and expected stage in the development and evolution of fundamentally new concepts. This specific issue is further discussed in the section on internal multiples.

### 3. Marine seismic exploration

In marine seismic exploration sources and receivers are located in the water column. The simplest reference medium that describes the marine seismic acquisition geometry is a half-space of water bounded by a free surface at the air–water interface. The reference Green operator,  $\mathbf{G}_0$ , consists of two parts:

$$\mathbf{G}_0 = \mathbf{G}_0^d + \mathbf{G}_0^{\text{FS}}, \quad (17)$$

where  $\mathbf{G}_0^d$  is the direct propagating, causal, whole-space Green operator in water and  $\mathbf{G}_0^{\text{FS}}$  is the additional part of the Green operator due to the presence of the free surface (see figure 3).  $\mathbf{G}_0^{\text{FS}}$  corresponds to a reflection off the free surface.

In the absence of a free surface, the reference medium is a whole space of water and  $\mathbf{G}_0^d$  is the reference Green operator. In this case, the forward series equation (7) describing the data is constructed from the direct propagating Green operator,  $\mathbf{G}_0^d$ , and the perturbation operator,  $\mathbf{V}$ . With our choice of reference medium, the perturbation operator characterizes the difference between earth properties and water; hence, the support of  $\mathbf{V}$  begins at the water bottom. With the free surface present, the forward series is constructed from  $\mathbf{G}_0 = \mathbf{G}_0^d + \mathbf{G}_0^{\text{FS}}$  and the same perturbation operator,  $\mathbf{V}$ . Hence,  $\mathbf{G}_0^{\text{FS}}$  is the sole difference between the forward series with and without the free surface; therefore  $\mathbf{G}_0^{\text{FS}}$  is responsible for generating those events that owe their existence to the presence of the free surface, i.e., ghosts and free-surface multiples. Ghosts are events that either start their history propagating up from the source and reflecting down from the free surface or end their history as the downgoing portion of the recorded wavefield at the receiver, having its last downward reflection at the free surface (see figure 4).

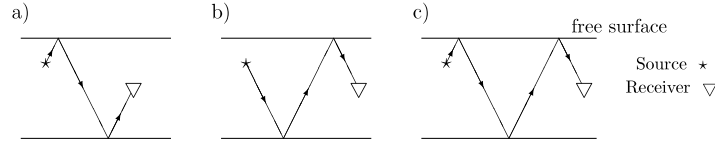


**Figure 4.** Examples of ghost events: (a) source ghost, (b) receiver ghost and (c) source–receiver ghost.

In the inverse series, equations (11)–(14), it is reasonable to infer that  $\mathbf{G}_0^{\text{FS}}$  will be responsible for all the extra tasks that inversion needs to perform when starting with data containing ghosts and free-surface multiples rather than data without those events. Those extra inverse tasks include deghosting and the removal of free-surface multiples. In the section on the free-surface demultiple subseries that follows, we describe how the extra portion of the reference Green operator due to the free surface,  $\mathbf{G}_0^{\text{FS}}$ , performs deghosting and free-surface multiple removal.

Once the events associated with the free surface are removed, the remaining measured field consists of primaries and internal multiples. For a marine experiment in the absence of a free surface, the scattered field,  $\Psi'_s$ , can be expressed as a series in terms of a reference medium consisting of a whole space of water, the reference Green operator,  $\mathbf{G}_0^{\text{d}}$ , and the perturbation,  $\mathbf{V}$ , as follows:

$$\begin{aligned}\Psi'_s &= \mathbf{G}_0^{\text{d}}\mathbf{V}\mathbf{G}_0^{\text{d}} + \mathbf{G}_0^{\text{d}}\mathbf{V}\mathbf{G}_0^{\text{d}}\mathbf{V}\mathbf{G}_0^{\text{d}} + \mathbf{G}_0^{\text{d}}\mathbf{V}\mathbf{G}_0^{\text{d}}\mathbf{V}\mathbf{G}_0^{\text{d}}\mathbf{V}\mathbf{G}_0^{\text{d}} + \dots \\ &= (\Psi'_s)_1 + (\Psi'_s)_2 + (\Psi'_s)_3 + \dots\end{aligned}\quad (18)$$

The values of  $\Psi'_s$  on the measurement surface,  $D'$ , are the data,  $D$ , collected in the absence of a free surface; i.e.,  $D'$  consists of primaries and internal multiples:

$$D' = D'_1 + D'_2 + D'_3 + \dots\quad (19)$$

$D'$  is the data  $D$  without free-surface events. Unfortunately, the free-space Green function,  $\mathbf{G}_0^{\text{d}}$ , does not separate into a part responsible for primaries and a part responsible for internal multiples. As a result, a totally new concept was required and introduced to separate the tasks associated with  $\mathbf{G}_0^{\text{d}}$  [5].

The forward scattering series (18) evaluated on the measurement surface describes data and *every* event in those data in terms of a series. Each term of the series corresponds to a sequence of *reference* medium propagations,  $\mathbf{G}_0^{\text{d}}$ , and scatterings off the perturbation,  $\mathbf{V}$ . A seismic event represents the measured arrival of energy that has experienced a specific set of actual reflections,  $R$ , and transmissions,  $T$ , at reflectors and propagations,  $p$ , governed by medium properties between reflectors. A complete description of an event would typically consist of a single term expression with all the actual episodes of  $R$ ,  $T$  and  $p$  in its history. The classification of an event in  $D'$  as a primary or as an internal multiple depends on the number and type of actual reflections that it has experienced. The scattering theory description of any specific event in  $D'$  requires an infinite series necessary to build the actual  $R$ ,  $T$  and  $p$  factors in terms of reference propagation,  $\mathbf{G}_0^{\text{d}}$ , and the perturbation operator,  $\mathbf{V}$ . That is,  $R$ ,  $T$  and  $p$  are non-linearly related to  $\mathbf{G}_0^{\text{d}}$  and  $\mathbf{V}$ . Even the simplest water bottom primary for which  $\mathbf{G}_0 = \mathbf{G}_0^{\text{d}}$  requires a series for its description in scattering theory (to produce the water bottom reflection,  $R$ , from an infinite series, non-linear in  $V$ ). We will illustrate this concept with a simple example later in this section. Hence, two chasms need to be bridged to determine the subseries that removes internal multiples. The first requires a map between primary and internal multiples in  $D'$  and their description in the language of forward scattering theory,

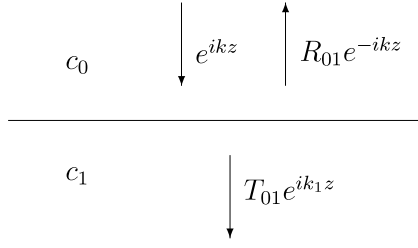


Figure 5. The 1D plane-wave normal incidence acoustic example.

$\mathbf{G}_0^d$  and  $\mathbf{V}$ ; the second requires a map between the construction of internal multiple events in the forward series and the removal of these events in the inverse series.

The internal multiple attenuation concept requires the construction of these two dictionaries: one relates seismic events to a forward scattering description, the second relates forward construction to inverse removal. The task separation strategy requires that those two maps be determined. Both of these multi-dimensional maps were originally inferred using arguments of physical intuition and mathematical reasonableness. Subsequently, Matson [18] provided a mathematically rigorous map of the relationship between seismic events and the forward scattering series for 1D constant density acoustic media that confirm the original intuitive arguments. Recent work by Nita *et al* [19] and Innanen and Weglein [20] extends that work to prestack analysis and absorptive media, respectively. The second map, relating forward construction and inverse removal, remains largely based on its original foundation. Recently, ten Kroode [15] presented a formal mathematical analysis for certain aspects of a forward to inverse internal multiple map (discussed in the previous section) based on a leading order definition of internal multiples and assumptions about the symmetry involved in the latter map. For the purpose of this article, we present only the key logical steps of the original arguments that lead to the required maps. The argument of the first map is presented here; the second map, relating forward construction and inverse removal, is presented in the next section.

To understand how the forward scattering series describes a particular event, it is useful to recall that the forward series for  $D'$  is a generalized Taylor series in the scattering operator,  $\mathbf{V}$  [21]. But what is the forward scattering subseries for a given event in  $D'$ ? Since a specific event consists of a set of actual  $R$ ,  $T$  and  $p$  factors, it is reasonable to start by asking how these individual factors are expressed in terms of the perturbation operator. Consider the simple example of one dimensional acoustic medium consisting of a single interface and a normal incidence plane wave,  $e^{ikz}$ , illustrated in figure 5.

Let the reference medium be a whole space with acoustic velocity,  $c_0$ . The actual and reference differential equations describing the actual and reference wavefields,  $P$  and  $P_0$ , are

$$\left[ \frac{d^2}{dz^2} + \frac{\omega^2}{c^2(z)} \right] P(z, \omega) = 0$$

and

$$\left[ \frac{d^2}{dz^2} + \frac{\omega^2}{c_0^2} \right] P_0(z, \omega) = 0,$$

where  $c(z)$  is the actual velocity.

The perturbation operator,  $\mathbf{V}$ , is

$$\mathbf{V} = \mathbf{L} - \mathbf{L}_0 = \frac{\omega^2}{c^2(z)} - \frac{\omega^2}{c_0^2}.$$

Characterize  $c(z)$  in terms of  $c_0$  and the variation in index of refraction,  $\alpha$ :

$$\frac{1}{c^2(z)} = \frac{1}{c_0^2} [1 - \alpha(z)].$$

In the lower half-space,

$$\frac{1}{c_1^2} = \frac{1}{c_0^2} [1 - \alpha_1],$$

$\alpha_1$  essentially represents the change in the perturbation operator at the interface (within a constant factor of  $-\omega^2/c_0^2$ ). The reflection and transmission coefficients and the transmitted wave propagating in the lower half-space are

$$R_{01} = \frac{c_1 - c_0}{c_1 + c_0},$$

$$T_{01} = \frac{2c_1}{c_1 + c_0}$$

and

$$P_1 = T_{01} \exp\left(i\frac{\omega}{c_1}z\right) = T_{01}p_1.$$

Using

$$c_1 \equiv \frac{c_0}{(1 - \alpha_1)^{1/2}} \approx c_0 \left[ 1 + \frac{1}{2}\alpha_1 + O(\alpha_1) \right],$$

these  $R$ ,  $T$  and  $p$  quantities are expandable as power series in the perturbation,  $\alpha_1$ :

$$R_{01} = \frac{1}{4}\alpha_1 + O(\alpha_1),$$

$$T_{01} = 1 + O(\alpha_1),$$

$$p_1 = \exp\left(i\frac{\omega}{c_1}z\right) = \exp\left(i\frac{\omega}{c_0}z\right) + O(\alpha_1)$$

$$= p_0 + O(\alpha_1).$$

Thus, to lowest order in an expansion in the local perturbation, the actual reflection is proportional to the local change in the perturbation, the transmission is proportional to 1 and the actual propagation is proportional to the reference propagation. An event in  $D'$  consists of a combination of  $R$ ,  $T$  and  $p$  episodes. The first term in the series that contributes to this event is determined by collecting the leading order contribution (in terms of the local change in the perturbation operator) from each  $R$ ,  $T$  and  $p$  factors in its history. Since the mathematical expression for an event is a *product* of all these actual  $R$ ,  $T$  and  $p$  factors, it follows that the lowest order contribution, in the powers of the perturbation operator, will equal the number of  $R$  factors in that event. The fact that the forward series, (18), is a power series in the perturbation operator allows us to identify the term in (19) that provides the first contribution to the construction of an event. Since by definition all primaries have only one  $R$  factor, their leading contribution comes with a single power of the perturbation operator from the first term of the series for  $D'$ . First order internal multiples, with three factors of reflection, have their leading contribution with three factors of the perturbation operator; hence, the leading order contribution to a first order internal multiple comes from the third term in the series for  $D'$ . All terms in the series beyond the first make second order and higher contributions for the construction of the  $R$ ,  $T$  and  $p$  factors of primaries. Similarly, all terms beyond the third provide higher order contributions for constructing the actual reflections, transmissions and propagations of first order internal multiples.

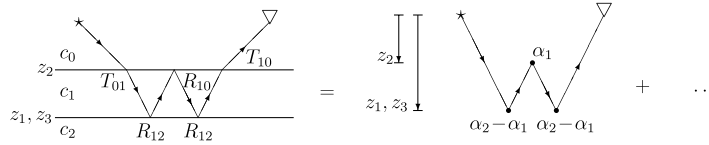


**Figure 6.** The left-hand member of this diagram represents a first order internal multiple; the right-hand member illustrates the first series contribution from  $D'_3$  towards the construction of the first order internal multiple.  $\alpha_1$  and  $\alpha_2 - \alpha_1$  are the perturbative contributions at the two reflectors;  $c_0, c_1$  and  $c_2$  are acoustic velocities where  $(1/c_2^2) = (1/c_0^2)(1 - \alpha_2)$  and  $(1/c_1^2) = (1/c_0^2)(1 - \alpha_1)$ .

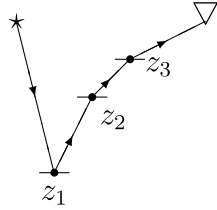


**Figure 7.** A diagram representing a portion of  $D'_3$  that makes a third order contribution to the construction of a primary.

How do we separate the part of the third term in the forward series that provides a third order contribution to primaries from the portion providing the leading term contribution to first order internal multiples? The key to the separation resides in recognizing that the three perturbative contributions in  $D'_3$  can be interpreted in the forward series as originating at the spatial *location* of reflectors. For a first order internal multiple the leading order contribution (illustrated on the right-hand member of figure 6) consists of perturbative contributions that can be interpreted as located at the spatial location (depth) of the three reflectors where reflections occur. For the example in figure 6, the three linear approximations to  $R_{12}$ ,  $R_{10}$  and  $R_{12}$ , that is,  $\alpha_2 - \alpha_1$ ,  $\alpha_1$  and  $\alpha_2 - \alpha_1$ , are located at depths  $z_1$ ,  $z_2$  and  $z_3$  where  $z_1 > z_2$  and  $z_3 > z_2$ . In this single layer example  $z_1$  is equal to  $z_3$ . In general,  $D'_3$  consists of the sum of all three perturbative contributions from any three reflectors at depths  $z_1$ ,  $z_2$  and  $z_3$ . The portion of  $D'_3$  where the three reflectors satisfy  $z_1 > z_2$  and  $z_3 > z_2$  corresponds to the leading order construction of a first order internal multiple involving those three reflectors. The parts of  $D'_3$  corresponding to the three perturbative contributions at reflectors that do not satisfy both of these inequalities provide third order contributions to the construction of primaries. A simple example is illustrated in figure 7.

The *sum* of *all* the contributions in  $D'_3$  that satisfy  $z_1 > z_2$  and  $z_3 > z_2$  for locations of the three successive perturbations is the sum of the leading contribution term for *all* first order internal multiples. The leading order term in the removal series for internal multiples of first order is cubic or third order in the measured data,  $D'$ . In the inverse series, 'order' means order in the data, not an asymptotic expansion and/or approximation. Similarly, second, third, ...,  $n$ th order internal multiples find their initial contribution in the fifth, seventh, ...,  $(2n + 1)$ th term of the forward series. We use the identified leading order contribution to all internal multiples of a given order in the forward series to infer a map to the corresponding leading order *removal* of all internal multiples of that order in the inverse series.

The forward map between the forward scattering series (7) and (8) for  $(\Psi_s)_m$  and the primaries and multiples of seismic reflection data works as follows. The scattering series builds the wavefield as a sum of terms with propagations  $\mathbf{G}_0$  and scattering off  $\mathbf{V}$ . Scattering



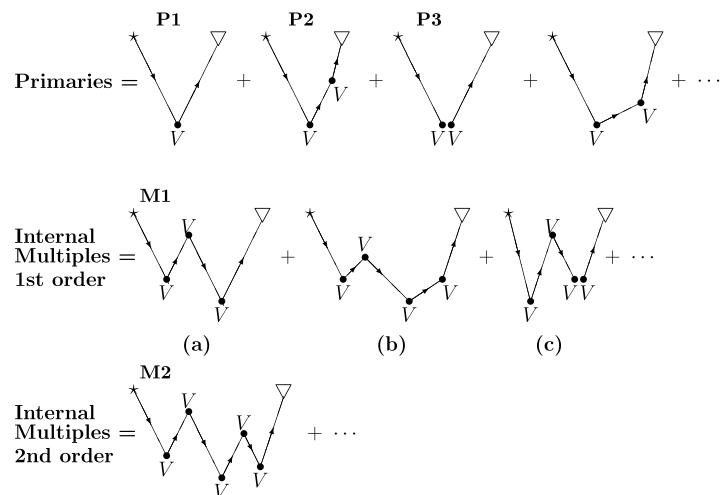


**Figure 8.** A scattering series description of primaries and internal multiples: P1—primary with one reflection; P2—primary with one reflection and one transmission; P3—primary with one reflection and a self-interaction; M1—first order internal multiple (one downward reflection); M2—second order internal multiple (two downward reflections).

occurs in all directions from the scattering point  $\mathbf{V}$  and the relative amplitude in a given direction is determined by the isotropy (or anisotropy) of the scattering operator. A scattering operator being anisotropic is distinct from physical anisotropy; the latter means that the wave speed in the actual medium at a point is a function of the direction of propagation of the wave at that point. A two parameter, variable velocity and density, acoustic isotropic medium has an anisotropic scattering operator (see (6)). In any case, since primaries and multiples are defined in terms of reflections, we propose that primaries and internal multiples will be distinguished by the number of reflection-like scatterings in their forward description, figure 8. A reflection-like scattering occurs when the incident wave moves away from the measurement surface towards the scattering point and the wave emerging from the scattering point moves towards the measurement surface.

Every reflection event in seismic data requires contributions from an infinite number of terms in the scattering theory description. Even with water velocity as the reference, and for events where the actual propagation medium is water, then the simplest primaries, i.e., the water bottom reflection, require an infinite number of contributions to take  $\mathbf{G}_0$  and  $\mathbf{V}$  into  $\mathbf{G}_0$  and  $R$ , where  $\mathbf{V}$  and  $R$  correspond to the perturbation operator and reflection coefficient at the water bottom, respectively. For a primary originating below the water bottom, the series has to deal with issues beyond turning the local value of  $\mathbf{V}$  into the local reflection coefficient,  $R$ . In the latter case, the reference Green function,  $\mathbf{G}_0$ , no longer corresponds to the propagation down to and back from the reflector ( $\mathbf{G} \neq \mathbf{G}_0$ ) and the terms in the series beyond the first are required to correct for timing errors and ignored transmission coefficients, in addition to taking  $\mathbf{V}$  into  $R$ .

The remarkable fact is that all primaries are constructed in the forward series by portions of every term in the series. The contributing part has one and only one upward reflection-like scattering. Furthermore, internal multiples of a given order have contributions from all terms that have exactly a number of downward reflection-like scatterings corresponding to the order of that internal multiple. The order of the internal multiple is defined by the number of downward reflections, independent of the location of the reflectors (see figure 8).

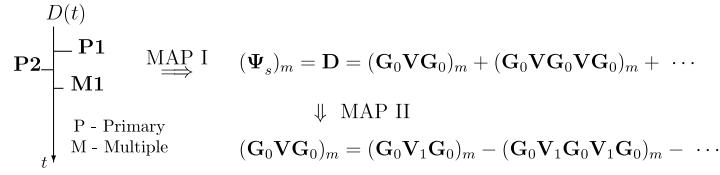


**Figure 9.** Maps for inverse scattering subseries. Map I takes seismic events to a scattering series description:  $D(t) = (\Psi_s)_m$  consists of primaries and multiples;  $(\Psi_s)_m = D(t)$  represents a forward series in terms of  $\mathbf{G}_0$  and  $\mathbf{V}$ . Map II takes forward construction of events to inverse processing of those events:  $(\mathbf{G}_0 \mathbf{V} \mathbf{G}_0)_m = (\mathbf{G}_0 \mathbf{V}_1 \mathbf{G}_0)_m - (\mathbf{G}_0 \mathbf{V}_1 \mathbf{G}_0 \mathbf{V}_1 \mathbf{G}_0)_m + \dots$ .

All internal multiples of first order begin their creation in the scattering series in the portion of the third term of  $(\Psi_s)_m$  with three reflection-like scatterings. All terms in the fourth and higher terms of  $(\Psi_s)_m$  that consist of three and only three reflection-like scatterings plus any number of transmission-like scatterings (e.g., event (b) in figure 8) and/or self-interactions (e.g., event (c) in figure 8) also contribute to the construction of first order internal multiples.

Further research in the scattering theory descriptions of seismic events is warranted and under way and will strengthen the first of the two key logic links (maps) required for developments of more effective and better understood task-specific inversion procedures.

#### 4. The inverse series and task separation: terms with coupled and uncoupled tasks

As discussed in section 3,  $\mathbf{G}_0^{\text{FS}}$  is the agent in the forward series that creates all events that come into existence due to the presence of the free surface (i.e., ghosts and free-surface multiples); when the inverse series starts with data that include free-surface-related events and, then inversion has additional tasks to perform on the way to constructing the perturbation,  $\mathbf{V}$  (i.e., deghosting and free-surface multiple removal); and, for the marine case, the forward and inverse reference Green operator,  $\mathbf{G}_0$ , consists of  $\mathbf{G}_0^{\text{d}}$  plus  $\mathbf{G}_0^{\text{FS}}$ . These three arguments taken together imply that, in the inverse series,  $\mathbf{G}_0^{\text{FS}}$  is the ‘removal operator’ for the surface-related events that it created in the forward series.

With that thought in mind, we will describe the deghosting and free-surface multiple removal subseries. The inverse series expansions, equations (11)–(14), consist of terms  $(\mathbf{G}_0 \mathbf{V}_n \mathbf{G}_0)_m$  with  $\mathbf{G}_0 = \mathbf{G}_0^{\text{d}} + \mathbf{G}_0^{\text{FS}}$ . Deghosting is realized by removing the two outside  $\mathbf{G}_0 = \mathbf{G}_0^{\text{d}} + \mathbf{G}_0^{\text{FS}}$  functions and replacing them with  $\mathbf{G}_0^{\text{d}}$ . The Green function  $\mathbf{G}_0^{\text{d}}$  represents a downgoing wave from source to  $\mathbf{V}$  and an upgoing wave from  $\mathbf{V}$  to the receiver (details are provided in section 5.4).

The source and receiver deghosted data,  $\tilde{D}$ , are represented by  $\tilde{D} = (\mathbf{G}_0^{\text{d}} \mathbf{V}_1 \mathbf{G}_0^{\text{d}})_m$ . After the deghosting operation, the objective is to remove the free-surface multiples from the deghosted data,  $\tilde{D}$ .

The terms in the inverse series expansions, (11)–(14), replacing  $D$  with input  $\tilde{D}$ , contain both  $\mathbf{G}_0^{\text{d}}$  and  $\mathbf{G}_0^{\text{FS}}$  between the operators  $\mathbf{V}_i$ . The outside  $\mathbf{G}_0^{\text{d}}$  s only indicate that the data have been source and receiver deghosted. The inner  $\mathbf{G}_0^{\text{d}}$  and  $\mathbf{G}_0^{\text{FS}}$  are where the four inversion tasks reside. If we consider the inverse scattering series and  $\mathbf{G}_0 = \mathbf{G}_0^{\text{d}} + \mathbf{G}_0^{\text{FS}}$  and if we assume that the data have been source and receiver deghosted (i.e.,  $\mathbf{G}_0^{\text{d}}$  replaces  $\mathbf{G}_0^{\text{FS}}$  on the outside contributions), then the terms in the series are of three types:

$$\begin{array}{l}
 \text{Type 1: } (\mathbf{G}_0^{\text{d}} \mathbf{V}_i \mathbf{G}_0^{\text{FS}} \mathbf{V}_j \mathbf{G}_0^{\text{FS}} \mathbf{V}_k \mathbf{G}_0^{\text{d}})_m \\
 \text{Type 2: } (\mathbf{G}_0^{\text{d}} \mathbf{V}_i \mathbf{G}_0^{\text{FS}} \mathbf{V}_j \mathbf{G}_0^{\text{d}} \mathbf{V}_k \mathbf{G}_0^{\text{d}})_m \\
 \text{Type 3: } (\mathbf{G}_0^{\text{d}} \mathbf{V}_i \mathbf{G}_0^{\text{d}} \mathbf{V}_j \mathbf{G}_0^{\text{d}} \mathbf{V}_k \mathbf{G}_0^{\text{d}})_m.
 \end{array}$$

We interpret these types of term from a task isolation point of view. Type 1 terms have only  $\mathbf{G}_0^{\text{FS}}$  between two  $\mathbf{V}_i, \mathbf{V}_j$  contributions; these terms when added to  $\tilde{D}$  remove free-surface multiples and perform no other task. Type 2 terms have both  $\mathbf{G}_0^{\text{d}}$  and  $\mathbf{G}_0^{\text{FS}}$  between two  $\mathbf{V}_i, \mathbf{V}_j$  contributions; these terms perform free-surface multiple removal *plus* a task associated with  $\mathbf{G}_0^{\text{d}}$ . Type 3 have only  $\mathbf{G}_0^{\text{d}}$  between two  $\mathbf{V}_i, \mathbf{V}_j$  contributions; these terms do not remove any free-surface multiples.

The idea behind task separated subseries is twofold:

- (1) isolate the terms in the overall series that perform a given task *as if no other tasks exist* (e.g., type 1 above) and
- (2) do not return to the original inverse series with its coupled tasks involving  $\mathbf{G}_0^{\text{FS}}$  and  $\mathbf{G}_0^{\text{d}}$ , but rather restart the problem with input data free of free-surface multiples,  $D'$ .

Collecting all type 1 terms we have

$$D'_1 \equiv \tilde{D} = (\mathbf{G}_0^{\text{d}} \mathbf{V}_1 \mathbf{G}_0^{\text{d}})_m \quad (11')$$

$$D'_2 = -(\mathbf{G}_0^{\text{d}} \mathbf{V}_1 \mathbf{G}_0^{\text{FS}} \mathbf{V}_1 \mathbf{G}_0^{\text{d}})_m \quad (12')$$

$$\begin{aligned} D'_3 = & -(\mathbf{G}_0^{\text{d}} \mathbf{V}_1 \mathbf{G}_0^{\text{FS}} \mathbf{V}_1 \mathbf{G}_0^{\text{FS}} \mathbf{V}_1 \mathbf{G}_0^{\text{d}})_m \\ & - (\mathbf{G}_0^{\text{d}} \mathbf{V}_1 \mathbf{G}_0^{\text{FS}} \mathbf{V}_2 \mathbf{G}_0^{\text{d}})_m \\ & - (\mathbf{G}_0^{\text{d}} \mathbf{V}_1 \mathbf{G}_0^{\text{FS}} \mathbf{V}_2 \mathbf{G}_0^{\text{d}})_m \end{aligned} \quad (13')$$

$\vdots$

$D'_3$  can be simplified as

$$D'_3 = +(\mathbf{G}_0^{\text{d}} \mathbf{V}_1 \mathbf{G}_0^{\text{FS}} \mathbf{V}_1 \mathbf{G}_0^{\text{FS}} \mathbf{V}_1 \mathbf{G}_0^{\text{d}})_m$$

(this reduction of (13') is not valid for type 2 or type 3 terms).  $D' = \sum_{i=1}^{\infty} D'_i$  are the deghosted and free-surface demultiplied data. The new free-surface demultiplied data,  $D'$ , consist of primaries and internal multiples and an inverse series for  $\mathbf{V} = \sum_{i=1}^{\infty} \mathbf{V}'_i$  where  $\mathbf{V}'_i$  is the portion of  $\mathbf{V}$  that is  $i$ th order in primaries and internal multiples. Collecting all type 3 terms:

$$D' = (\mathbf{G}_0^{\text{d}} \mathbf{V}'_1 \mathbf{G}_0^{\text{d}})_m \quad (11'')$$

$$(\mathbf{G}_0^{\text{d}} \mathbf{V}'_2 \mathbf{G}_0^{\text{d}})_m = -(\mathbf{G}_0^{\text{d}} \mathbf{V}'_1 \mathbf{G}_0^{\text{d}} \mathbf{V}'_1 \mathbf{G}_0^{\text{d}})_m \quad (12'')$$

$$\begin{aligned} (\mathbf{G}_0^{\text{d}} \mathbf{V}'_3 \mathbf{G}_0^{\text{d}})_m = & -(\mathbf{G}_0^{\text{d}} \mathbf{V}'_1 \mathbf{G}_0^{\text{d}} \mathbf{V}'_1 \mathbf{G}_0^{\text{d}} \mathbf{V}'_1 \mathbf{G}_0^{\text{d}})_m \\ & - (\mathbf{G}_0^{\text{d}} \mathbf{V}'_1 \mathbf{G}_0^{\text{d}} \mathbf{V}'_2 \mathbf{G}_0^{\text{d}})_m \\ & - (\mathbf{G}_0^{\text{d}} \mathbf{V}'_2 \mathbf{G}_0^{\text{d}} \mathbf{V}'_1 \mathbf{G}_0^{\text{d}})_m \end{aligned} \quad (13'')$$

$\vdots$

When the free surface is absent,  $\mathbf{G}_0^{\text{d}}$  creates primaries and internal multiples in the forward series and is responsible for carrying out all inverse tasks on those same events in the inverse series.

We repeat this process seeking to isolate terms that only 'care about' the responsibility of  $\mathbf{G}_0^{\text{d}}$  towards removing internal multiples. No coupled task terms that involve both internal multiples and primaries are included. After the internal multiples attenuation task is accomplished we restart the problem once again and write an inverse series whose input consists only of primaries. This task isolation and restarting of the definition of the inversion

procedure strategy have several advantages over staying with the original series. Those advantages include the recognition that a task that has already been accomplished is a form of new information and makes the subsequent and progressively more difficult tasks in our list considerably less daunting compared to the original all-inclusive data series approach. For example, after removing multiples with a reference medium of water speed, it is easier to estimate a variable background to aid convergence for subsequent tasks whose subseries might benefit from that advantage. Note that the  $\mathbf{V}$  represents the difference between water and earth properties and can be expressed as  $\mathbf{V} = \sum_{i=1}^{\infty} \mathbf{V}_i$  and  $\mathbf{V} = \sum_{i=1}^{\infty} \mathbf{V}'_i$ . However,  $\mathbf{V}_i \neq \mathbf{V}'_i$  since  $\mathbf{V}_i$  assumes that the data are  $D$  (primaries and all multiples) and  $\mathbf{V}'_i$  assumes that the data are  $D'$  (primaries and only internal multiples). In other words,  $\mathbf{V}_1$  is linear in all primaries and free-surface and internal multiples, while  $\mathbf{V}'_1$  is linear in all primaries and internal multiples only.

## 5. An analysis of the earth model type and the inverse series and subseries

### 5.1. Model type and the inverse series

To invert for medium properties requires choosing a set of parameters that you seek to identify. The chosen set of parameters (e.g., P and S wave velocity and density) defines an earth model type (e.g., acoustic, elastic, isotropic, anisotropic earth) and the details of the inverse series will depend on that choice. Choosing an earth model type defines the form of  $\mathbf{L}$ ,  $\mathbf{L}_0$  and  $\mathbf{V}$ . On the way towards identifying the earth properties (for a given model type), intermediate tasks are performed, such as the removal of free-surface and internal multiples and the location of reflectors in space.

It will be shown below that the free-surface and internal multiple attenuation subseries not only do not require subsurface information for a given model type, but are even independent of the earth model type itself for a very large class of models. The meaning of model type-independent task-specific subseries is that the defined task is achievable with precisely the same algorithm for an entire class of earth model types. The members of the model type class that we are considering satisfy the convolution theorem and include acoustic, elastic and certain anelastic media.

In this section, we provide a more general and complete formalism for the inverse series, and especially the subseries, than has appeared in the literature to date. That formalism allows us to examine the issue of model type and inverse scattering objectives. When we discuss the imaging and inversion subseries in section 8, we use this general formalism as a framework for defining and addressing the new challenges that we face in developing subseries that perform imaging at depth without the velocity and inverting large contrast complex targets. All inverse methods for identifying medium properties require specification of the parameters to be determined, i.e., of the assumed earth model type that has generated the scattered wavefield. To understand how the free-surface multiple removal and internal multiple attenuation task-specific subseries avoid this requirement (and to understand under what circumstances the imaging subseries would avoid that requirement as well), it is instructive to examine the mathematical physics and logic behind the classic inverse series and see precisely the role that model type plays in the derivation.

References for the inverse series include [4, 10, 12, 13]. The inverse series paper by Razavy [12] is a lucid and important paper relevant to seismic exploration. In that paper, Razavy considers a normal plane wave incident on a one dimensional acoustic medium. We follow Razavy's development to see precisely how model type enters and to glean further physical insight from the mathematical procedure. Then we introduce a perturbation operator,  $\mathbf{V}$ ,

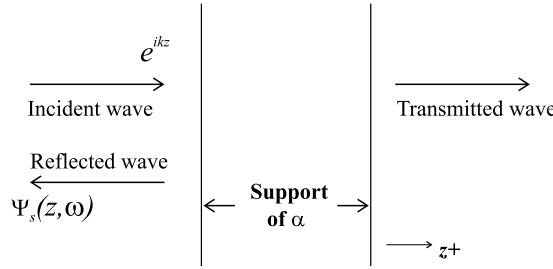


Figure 10. The scattering experiment: a plane wave incident upon the perturbation,  $\alpha$ .

general enough in structure to accommodate the entire class of earth model types under consideration.

Finally, if a process (i.e., a subseries) can be performed without specifying how  $\mathbf{V}$  depends on the earth property changes (i.e., what set of earth properties are assumed to vary inside  $\mathbf{V}$ ), then the process itself is independent of earth model type.

5.2. Inverse series for a 1D acoustic constant density medium

Start with the 1D variable velocity, constant density acoustic wave equation, where  $c(z)$  is the wave speed and  $\Psi(z, t)$  is a pressure field at location  $z$  at time  $t$ . The equation that  $\Psi(z, t)$  satisfies is

$$\left( \frac{\partial^2}{\partial z^2} - \frac{1}{c^2(z)} \frac{\partial^2}{\partial t^2} \right) \Psi(z, t) = 0 \tag{20}$$

and after a temporal Fourier transform,  $t \rightarrow \omega$ ,

$$\left( \frac{d^2}{dz^2} + \frac{\omega^2}{c^2(z)} \right) \Psi(z, \omega) = 0. \tag{21}$$

Characterize the velocity configuration  $c(z)$  in terms of a reference velocity,  $c_0$ , and perturbation,  $\alpha$ :

$$\frac{1}{c^2(z)} = \frac{1}{c_0^2} (1 - \alpha(z)). \tag{22}$$

The experiment consists of a plane wave  $e^{ikz}$  where  $k = \omega/c_0$  incident upon  $\alpha(z)$  from the left (see figure 10). Assume here that  $\alpha$  has compact support and that the incident wave approaches  $\alpha$  from the same side as the scattered field is measured.

Let  $b(k)$  denote the overall reflection coefficient for  $\alpha(z)$ . It is determined from the reflection data at a given frequency  $\omega$ . Then  $e^{ikz}$  and  $b(k)e^{-ikz}$  are the incident and the reflected waves respectively. Rewrite (21) and (22) and the incident wave boundary condition as an integral equation:

$$\Psi(z, \omega) = e^{ikz} + \frac{1}{2ik} \int e^{ik|z-z'|} k^2 \alpha(z') \Psi(z', \omega) dz' \tag{23}$$

and define the scattered field  $\Psi_s$ :

$$\Psi_s(z, \omega) \equiv \Psi(z, \omega) - e^{ikz}.$$

Also, define the  $T$  matrix:

$$T(p, k) \equiv \int e^{-ipz} \alpha(z) \Psi(z, k) dz \tag{24}$$

and the Fourier sandwich of the parameter,  $\alpha$ :

$$\alpha(p, k) \equiv \int e^{-ipz} \alpha(z) e^{ikz} dz.$$

The scattered field,  $\Psi_s$ , takes the form

$$\Psi_s(z, \omega) = b(k) e^{-ikz} \quad (25)$$

for values of  $z$  less than the support of  $\alpha(z)$ . From (23) to (25) it follows that

$$T(-k, k) \frac{k}{2i} = b(k). \quad (26)$$

Multiply (23) by  $\alpha(z)$  and then Fourier transform over  $z$  to find

$$T(p, k) = \alpha(p, k) - k^2 \int_{-\infty}^{\infty} \frac{\alpha(p, q) T(q, k)}{q^2 - k^2 - i\epsilon} dq \quad (27)$$

where  $p$  is the Fourier conjugate of  $z$  and use has been made of the bilinear form of the Green function. Razavy [12] also derives another integral equation by interchanging the roles of unperturbed and perturbed operators, with  $\mathbf{L}_0$  viewed as a perturbation of  $-\mathbf{V}$  on a reference operator  $\mathbf{L}$ :

$$\alpha(p, k) = T(p, k) + k^2 \int_{-\infty}^{\infty} \frac{T^*(k, q) T(p, q)}{q^2 - k^2 - i\epsilon} dq. \quad (28)$$

Finally, define  $W(k)$  as essentially the Fourier transform of the sought after perturbation,  $\alpha$ :

$$W(k) \equiv \alpha(-k, k) = \int_{-\infty}^{\infty} e^{2ikz} \alpha(z) dz \quad (29)$$

and recognize that predicting  $W(k)$  for all  $k$  produces  $\alpha(z)$ .

From (28), we find, after setting  $p = -k$ ,

$$W(k) = \alpha(-k, k) = T(-k, k) + k^2 \int_{-\infty}^{\infty} \frac{T^*(k, q) T(-k, q)}{q^2 - k^2 - i\epsilon} dq. \quad (30)$$

The left-hand member of (30) is the desired solution,  $W(k)$ , but the right-hand member requires both  $T(-k, k)$  that we determine from  $2ib(k)/k$  and  $T^*(k, q)T(-k, q)$  for all  $q$ .

We cannot directly determine  $T(k, q)$  for all  $q$  from measurements outside  $\alpha$ —only  $T(-k, k)$  from reflection data and  $T(k, k)$  from transmission data. If we could determine  $T(k, q)$  for all  $q$ , then (30) would represent a *closed form* solution to the (multi-dimensional) inverse problem. If  $T(-k, k)$  and  $T(k, k)$  relate to the reflection and transmission coefficients, respectively, then what does  $T(k, q)$  mean for all  $q$ ?

Let us start with the integral form for the scattered field

$$\Psi_s(z, k) = \frac{1}{2\pi} \int \int \frac{e^{ik'(z-z')}}{k^2 - k'^2 - i\epsilon} dk' k^2 \alpha(z') \Psi(z', k) dz' \quad (31)$$

and Fourier transform (31) going from the configuration space variable,  $z$ , to the wavenumber,  $p$ , to find

$$\Psi_s(p, k) = \int \int \frac{\delta(k' - p) e^{-ik'z'}}{k^2 - k'^2 - i\epsilon} dk' k^2 \alpha(z') \Psi(z', k) dz' \quad (32)$$

and integrate over  $k'$  to find

$$\Psi_s(p, k) = \frac{k^2}{k^2 - p^2 - i\epsilon} \int e^{-ipz'} \alpha(z') \Psi(z', k) dz'. \quad (33)$$

The integral in (33) is recognized from (24) as

$$\Psi_s(p, k) = k^2 \frac{T(p, k)}{k^2 - p^2 - i\epsilon}. \quad (34)$$

Therefore to determine  $T(p, k)$  for all  $p$  for any  $k$  is to determine  $\Psi_s(p, k)$  for all  $p$  and any  $k$  ( $k = \omega/c_0$ ). But to find  $\Psi_s(p, k)$  from  $\Psi_s(z, k)$  you need to compute

$$\int_{-\infty}^{\infty} e^{-ipz} \Psi_s(z, k) dz, \quad (35)$$

which means that it requires  $\Psi_s(z, k)$  at every  $z$  (not just at the measurement surface, i.e., a fixed  $z$  value outside of  $\alpha$ ). Hence (30) would provide  $W(k)$  and therefore  $\alpha(z)$ , if we provide not only reflection data,  $b(k) = T(-k, k)2i/k$ , but also the scattered field,  $\Psi_s$ , at all depths,  $z$ .

Since knowledge of the scattered field,  $\Psi_s$  (and, hence, the total field), at all  $z$  could be used in (21) to directly compute  $c(z)$  at all  $z$ , there is not much point or value in treating (30) in its pristine form as a complete and direct inverse solution.

Moses [10] first presented a way around this dilemma. His thinking resulted in the inverse scattering series and consisted of two necessary and sufficient ingredients: (1) model type combined with (2) a solution for  $\alpha(z)$  and all quantities that depend on  $\alpha$ , order by order in the data,  $b(k)$ .

Expand  $\alpha(z)$  as a series in orders of the measured data:

$$\alpha = \alpha_1 + \alpha_2 + \alpha_3 + \dots = \sum_{n=1}^{\infty} \alpha_n \quad (36)$$

where  $\alpha_n$  is  $n$ th order in the data  $D$ . When the inaccessible  $T(p, k)$ ,  $|p| \neq |k|$ , are ignored, (30) becomes the Born–Heitler approximation and a comparison to the inverse Born approximation (the Born approximation ignores the entire second term of the right-hand member of (30)) was analysed in [22].

It follows that all quantities that are power series (starting with power one) in  $\alpha$  are also power series in the measured data:

$$T(p, k) = T_1(p, k) + T_2(p, k) + \dots, \quad (37)$$

$$W(k) = W_1(k) + W_2(k) + \dots, \quad (38)$$

$$\alpha(p, k) = \alpha_1(p, k) + \alpha_2(p, k) + \dots. \quad (39)$$

The model type (i.e., acoustic constant density variable velocity in the equation for pressure) provides a key relationship for the perturbation,  $V = k^2\alpha$ :

$$\alpha(p, k) = W\left(\frac{k-p}{2}\right) \quad (40)$$

that constrains the Fourier sandwich,  $\alpha(p, k)$ , to be a function of only the difference between  $k$  and  $p$ . This model type, combined with order by order analysis of the construction of  $T(p, k)$  for  $p \neq k$  required by the series, provides precisely what we need to solve for  $\alpha(z)$ .

Starting with the measured data,  $b(k)$ , and substituting  $W = \sum W_n$ ,  $T = \sum T_n$  from (37) and (38) into (30), we find

$$\sum_{n=1}^{\infty} W_n(k) = \frac{2i}{k} b(k) + k^2 \int \frac{dq}{q^2 - k^2 - i\epsilon} \left( \sum_{n=1}^{\infty} T_n^* \sum_{n=1}^{\infty} T_n \right). \quad (41)$$

To first order in the data,  $b(k)$ ,  $k > 0$  (note that  $b^*(+k) = b(-k)$ ,  $k > 0$ ), equation (41) provides

$$W_1(k) = \frac{2i}{k} b(k) \quad (42)$$

and (42) determines  $W_1(k)$  for all  $k$ . From (42) together with (29) to first order in the data

$$W_1(k) = \alpha_1(-k, k) = \int_{-\infty}^{\infty} \alpha_1(z) e^{2ikz} dz, \quad (43)$$

we find  $\alpha_1(z)$ . The next step towards our objective of constructing  $\alpha(z)$  is to find  $\alpha_2(z)$ .

From  $W_1(k)$  we can determine  $W_1(k-p)/2$  for all  $k$  and  $p$  and from (40) to first order in the data

$$\alpha_1(p, k) = W_1\left(\frac{k-p}{2}\right), \quad (44)$$

which in turn provides  $\alpha_1(p, k)$  for all  $p, k$ . The relationship (44) is model type in action as seen by exploiting the acoustic model with variable velocity and the constant density assumption.

Next, (28) provides to first order  $\alpha_1(p, k) = T_1(p, k)$  for all  $p$  and  $k$ . This is the critically important argument that builds the scattered field at all depths, order by order, in the measured values of the scattered field. Substituting the  $\alpha_1, T_1$  relationship into (30), we find the second order relationship in the data:

$$W_2(k) = k^2 \int_{-\infty}^{\infty} \frac{dq}{q^2 - k^2 - i\epsilon} T_1^*(k, q) T_1(-k, q) \quad (45)$$

and

$$W_2(k) = \int_{-\infty}^{\infty} e^{2ikz} \alpha_2(z) dz. \quad (46)$$

After finding  $\alpha_2(z)$  we can repeat the steps to determine the total  $\alpha$  order by order:

$$\alpha = \alpha_1(z) + \alpha_2(z) + \dots$$

Order by order arguments and the model type allow

$$T_1(p, k) = \alpha_1(p, k)$$

for all  $p$  and  $k$ , although, as we observed, the higher order relationships between  $T_i$  and  $\alpha_i$  are more complicated:

$$\begin{aligned} T_2(p, k) &\neq \alpha_2(p, k) \\ T_3(p, k) &\neq \alpha_3(p, k) \\ &\vdots \\ T_n(p, k) &\neq \alpha_n(p, k). \end{aligned}$$

From a physics and information content point of view, what has happened? The data  $D$  collected at e.g.  $z = 0$ ,  $\Psi_s(z = 0, \omega)$  determine  $b(k)$ . This in turn allows the construction of  $T(p, k)$ , where  $k = \omega/c_0$  for all  $p$  order by order in the data. Hence the required scattered wavefield at depth, represented by  $T(p, k)$  for all  $p$ , (30), is constructed order by order, for a single temporal frequency,  $\omega$ , using the model type constraint. The data at one depth for all frequencies are traded for the wavefield at all depths at one frequency. This observation, that in constructing the perturbation,  $\alpha(z)$ , order by order in the data, the actual wavefield at depth is constructed, represents an alternate path or strategy for seismic inversion (see [23]).

If the inverse series makes these model type requirements for its construction, how do the free-surface removal and internal multiple attenuation subseries work independently of earth model type? What can we anticipate about the attitude of the imaging and inversion at depth subseries with respect to these model type dependence issues?



### 5.3. The operator $\mathbf{V}$ for a class of earth model types

Consider once again the variable velocity, variable density acoustic wave equation

$$\left(\frac{\omega^2}{K} + \nabla \cdot \frac{1}{\rho} \nabla\right) P = 0 \quad (47)$$

where  $K$  and  $\rho$  are the bulk modulus and density and can be written in terms of reference values  $K_0$  and  $\rho_0$ , and perturbations  $a_1$  and  $a_2$ :

$$\frac{1}{K} = \frac{1}{K_0}(1 + a_1) \quad \frac{1}{\rho} = \frac{1}{\rho_0}(1 + a_2)$$

$$\mathbf{L}_0 = \frac{\omega^2}{K_0} + \nabla \cdot \frac{1}{\rho_0} \nabla \quad (48)$$

$$\mathbf{V} = \frac{\omega^2}{K_0} a_1(\mathbf{r}) + \left(\nabla \cdot \frac{a_2(\mathbf{r})}{\rho_0} \nabla\right). \quad (49)$$

We will assume a 2D earth with line sources and receivers (the 3D generalization is straightforward). A Fourier sandwich of this  $\mathbf{V}$  is

$$V(\mathbf{p}, \mathbf{k}; \omega) = \int e^{-i\mathbf{p}\cdot\mathbf{r}} \mathbf{V} e^{i\mathbf{k}\cdot\mathbf{r}} d\mathbf{r} = \frac{\omega^2}{K_0} a_1(\mathbf{k} - \mathbf{p}) + \frac{\mathbf{k} \cdot \mathbf{p}}{\rho_0} a_2(\mathbf{k} - \mathbf{p}) \quad (50)$$

where  $\mathbf{p}$  and  $\mathbf{k}$  are arbitrary 2D vectors. The Green theorem and the compact support of  $a_1$  and  $a_2$  are used in deriving (50) from (49). For an isotropic elastic model, (50) generalizes for  $V^{\text{PP}}$  (see [3, 24, 25]):

$$V^{\text{PP}}(\mathbf{p}, \mathbf{k}; \omega) = \frac{\omega^2}{K_0} a_1(\mathbf{k} - \mathbf{p}) + \frac{\mathbf{k} \cdot \mathbf{p}}{\rho_0} a_2(\mathbf{k} - \mathbf{p}) - \frac{2\beta_0^2}{\omega^2} |\mathbf{k} \times \mathbf{p}|^2 a_3(\mathbf{k} - \mathbf{p}) \quad (51)$$

where  $a_3$  is the relative change in shear modulus and  $\beta_0$  is the shear velocity in the reference medium.

The inverse series procedure can be extended for perturbation operators (50) or (51), but the detail will differ for these two models. The model type and order by order arguments still hold. Hence the 2D (or 3D) general perturbative form will be

$$V(\mathbf{p}, \mathbf{k}; \omega) = V_1(\mathbf{p}, \mathbf{k}; \omega) + \dots$$

where  $\mathbf{p}$  and  $\mathbf{k}$  are 2D (or 3D) independent wavevectors that can accommodate a set of earth model types that include acoustic, elastic and certain anelastic forms. For example:

- acoustic (constant density):

$$V = \frac{\omega^2}{\alpha_0^2} a_1,$$

- acoustic (variable density):

$$V = \frac{\omega^2}{\alpha_0^2} a_1 + \mathbf{k} \cdot \mathbf{k}' a_2,$$

- elastic (isotropic, P–P):

$$V = \frac{\omega^2}{\alpha_0^2} a_1 + \mathbf{k} \cdot \mathbf{k}' a_2 - 2 \frac{\beta_0^2}{\omega^2} |\mathbf{k} \times \mathbf{k}'|^2 a_3,$$

where  $\alpha_0$  is the compressional wave velocity,  $a_1$  is the relative change in the bulk modulus,  $a_2$  is the relative change in density and  $a_3$  is the relative change in shear modulus.

What can we compute in the inverse series without specifying how  $V$  depends on  $(a_1)$ ,  $(a_1, a_2)$ , ...? If we can achieve a task in the inverse series without specifying what parameters  $V$  depends on, then that task can be attained with the identical algorithm *independently* of the earth model type.

#### 5.4. Free-surface multiple removal subseries and model type independence

In (11)–(14), we presented the general inverse scattering series without specifying the nature of the reference medium that determines  $\mathbf{L}_0$  and  $\mathbf{G}_0$  and the class of earth model types that relate to the form of  $\mathbf{L}$ ,  $\mathbf{L}_0$  and  $\mathbf{V}$ . In this section, we present the explicit inverse scattering series for the case of marine acquisition geometry. This will also allow the issue of model type independence to be analysed in the context of marine exploration.

The reference medium is a half-space, with the acoustic properties of water, bounded by a free surface at the air–water interface, located at  $z = 0$ . We consider a 2D medium and assume that a line source and receivers are located at  $(x_s, \epsilon_s)$  and  $(x_g, \epsilon_g)$ , where  $\epsilon_s$  and  $\epsilon_g$  are the depths below the free surface of the source and receivers, respectively.

The reference operator,  $\mathbf{L}_0$ , satisfies

$$\begin{aligned} \mathbf{L}_0 G_0 &= \left( \frac{\nabla^2}{\rho_0} + \frac{\omega^2}{K_0} \right) G_0(x, z, x', z'; \omega) \\ &= -\delta(x - x') \{ \delta(z - z') - \delta(z + z') \}, \end{aligned} \quad (52)$$

where  $\rho_0$  and  $K_0$  are the density and bulk modulus of water, respectively. The two terms in the right member of (52) correspond to the source located at  $(x', z')$  and the image of this source, across the free surface, at  $(x', -z')$ , respectively;  $(x, z)$  is any point in 2D space.

The actual medium is a general earth model with associated wave operator  $\mathbf{L}$  and Green function  $G$ . Fourier transforming (52) with respect to  $x$ , we find

$$\left[ \frac{1}{\rho_0} \frac{d^2}{dz^2} + \frac{q^2}{\rho_0} \right] G_0(k_x, z, x', z'; \omega) = -\frac{1}{(2\pi)^{1/2}} e^{-ik_x x'} \{ \delta(z - z') - \delta(z + z') \}. \quad (53)$$

The causal solution of (53) is

$$G_0(k_x, z, x', z'; \omega) = \frac{\rho_0}{\sqrt{2\pi}} \frac{e^{-ik_x x'}}{-2iq} (e^{iq|z-z'|} - e^{iq|z+z'|}), \quad (54)$$

where the vertical wavenumber,  $q$ , is defined as

$$q = \text{sgn}(\omega) \sqrt{(\omega/c_0)^2 - k_x^2},$$

and  $c_0$  is the acoustic velocity of water:

$$c_0 = \sqrt{K_0/\rho_0}.$$

With  $G_0$  given by (54), the linear form, (11), can be written as

$$D(k_g, \epsilon_g, k_s, \epsilon_s; \omega) = \frac{\rho_0^2}{q_g q_s} \sin(q_g \epsilon_g) \sin(q_s \epsilon_s) V_1(k_g, q_g, k_s, q_s; \omega), \quad (55)$$

where  $V(\mathbf{k}_g, \mathbf{k}_s, \omega) = V_1(\mathbf{k}_g, \mathbf{k}_s, \omega) + V_2(\mathbf{k}_g, \mathbf{k}_s, \omega) + \dots$  and  $\mathbf{k}_g, \mathbf{k}_s$  are arbitrary two dimensional vectors defined as

$$\mathbf{k}_g = (k_g, -q_g), \quad \mathbf{k}_s = (k_s, +q_s).$$

The variable  $k_z$  is defined as

$$k_z = -(q_g + q_s),$$

where

$$q_g = \text{sgn}(\omega) \sqrt{(\omega/c_0)^2 - k_g^2}, \quad (56)$$

and

$$q_s = \text{sgn}(\omega) \sqrt{(\omega/c_0)^2 - k_s^2}. \quad (57)$$

The first term in the inverse series in two dimensions (11') in terms of deghosted data,  $\tilde{D}$  is

$$\frac{D}{(e^{2iq_g\epsilon_g} - 1)(e^{2iq_s\epsilon_s} - 1)} = \mathbf{G}_0^d \mathbf{V}_1 \mathbf{G}_0^d = \tilde{D}(k_g, \epsilon_g, k_s, \epsilon_s; \omega). \quad (58)$$

Using the bilinear form for  $\mathbf{G}_0^d$  on both sides of  $\mathbf{V}_1$  in (58) and Fourier transforming both sides of this equation with respect to  $x_s$  and  $x_g$  we find

$$e^{iq_g\epsilon_g} e^{iq_s\epsilon_s} \frac{V_1(\mathbf{k}_g, \mathbf{k}_s; \omega)}{q_g q_s} = \tilde{D}(k_g, \epsilon_g, k_s, \epsilon_s; \omega) \quad (59)$$

where  $\mathbf{k}_g$  and  $\mathbf{k}_s$  are now constrained by  $|\mathbf{k}_g| = |\mathbf{k}_s| = \omega/c_0$  in the left-hand member of (59).

In a 2D world, only the three dimensional projection of the five dimensional  $V_1(\mathbf{p}, \mathbf{k}; \omega)$  is recoverable from the surface measurements  $D(k_g, \epsilon_g, k_s, \epsilon_s; \omega)$  which is a function of three variables, as well. It is important to recognize that you cannot determine  $\mathbf{V}_1$  for a general operator  $V_1(\mathbf{r}_1, \mathbf{r}_2; \omega)$  or  $V_1(\mathbf{k}', \mathbf{k}; \omega)$  from surface measurements and only the three dimensional projection of  $V_1(\mathbf{k}', \mathbf{k}; \omega)$  with  $|\mathbf{k}| = |\mathbf{k}'| = \omega/c_0$  is recoverable. However, this three dimensional projection of  $\mathbf{V}_1$  is more than enough to compute the first order changes,  $a_i^1(\mathbf{r})$ , for a given earth model type in any number of two dimensional earth model parameters ( $a_i^1$  is the first order approximation to  $a_i(\mathbf{r})$ ). After solving for  $a_1^1(\mathbf{r})$ ,  $a_2^1(\mathbf{r})$ ,  $a_3^1(\mathbf{r})$ ,  $\dots$ , you could then use  $a_1^1, a_2^1, a_3^1, \dots$  to compute  $V_1(\mathbf{k}', \mathbf{k}, \omega)$  for all  $\mathbf{k}', \mathbf{k}$  and  $\omega$ . This is the direct extension of the first step of the Moses [10] procedure where model type is exploited.

$\mathbf{V}_2$  is computed from  $\mathbf{V}_1$  using (12):

$$(\mathbf{G}_0 \mathbf{V}_2 \mathbf{G}_0)_m = -(\mathbf{G}_0 \mathbf{V}_1 \mathbf{G}_0 \mathbf{V}_1 \mathbf{G}_0)_m \quad (60)$$

and is written in terms of the general  $V_1$  form

$$\begin{aligned} V_2(\mathbf{k}'_g, \mathbf{k}_s, \omega) &= -\frac{1}{2\pi} \int \int \int \int e^{-i\mathbf{k}'_g \cdot \mathbf{r}_1} V_1(\mathbf{r}_1, \mathbf{r}_2, \omega) G_0(\mathbf{r}_2, \mathbf{r}_3; \omega) \\ &\quad \times V_1(\mathbf{r}_3, \mathbf{r}_4; \omega) e^{i\mathbf{k}_s \cdot \mathbf{r}_4} d\mathbf{r}_1 d\mathbf{r}_2 d\mathbf{r}_3 d\mathbf{r}_4 \\ &= -\int \int V_1(\mathbf{k}'_g, \mathbf{r}_2, \omega) G_0(\mathbf{r}_2, \mathbf{r}_3, \omega) V_1(\mathbf{r}_3, \mathbf{k}_s, \omega) d\mathbf{r}_2 d\mathbf{r}_3. \end{aligned} \quad (61)$$

Expressing  $G_0$  as a Fourier transform over  $x_2 - x_3$ , we find

$$G_0(x_2 - x_3, z_2, z_3; \omega) = \frac{1}{\sqrt{2\pi}} \int dk G_0(k, z_2, z_3; \omega) e^{ik(x_2 - x_3)} \quad (62)$$

and

$$G_0(k, z_2, z_3; \omega) = \frac{1}{\sqrt{2\pi}} \int e^{-ikx} dx G_0(x, z_2, z_3; \omega). \quad (63)$$

For  $G_0 = G_0^d$ , (63) reduces to

$$G_0^d(k, z_2, z_3; \omega) = -\frac{e^{iq|z_2 - z_3|}}{2iq} \quad (64)$$

where

$$q = \sqrt{\left(\frac{\omega}{c_0}\right)^2 - k^2}.$$

For the marine case where there is a free surface, the Green function  $G_0$  satisfies

$$\left(\nabla^2 + \frac{\omega^2}{c_0^2}\right) G_0 = -(\delta(\mathbf{r}_2 - \mathbf{r}_3) - \delta(\mathbf{r}_2 - \mathbf{r}_3^i)) \quad (65)$$

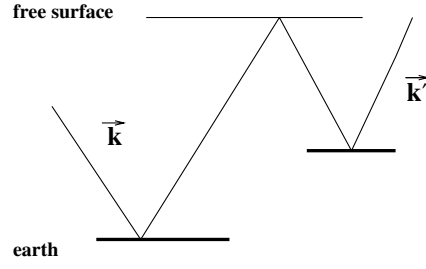


Figure 11. An illustration of  $\mathbf{k}$  and  $\mathbf{k}'$ .

and a Fourier transform over  $x_2 - x_3$  yields

$$\left( \frac{d^2}{dz_2^2} - k_x^2 + \frac{\omega^2}{c_0^2} \right) G_0 = -(\delta(z_2 - z_3) - \delta(z_2 - z_3^i)) \quad (66)$$

where  $z_3^i$  is the image across the free surface of  $z_3$  (with the free surface at  $z = 0$ ,  $z_3^i = -z_3$ ). The causal solution to (66) is

$$G_0(k_x, z_2, z_3, \omega) = -\frac{e^{iq|z_2-z_3|} - e^{iq|z_2+z_3|}}{2iq} = G_0^d + G_0^{\text{FS}}.$$

The contribution to  $\mathbf{V}_2$  from the additional portion of the Green function due to the free surface,  $G_0^{\text{FS}} = \frac{e^{iq|z_2+z_3|}}{2iq}$ , will be from (61)

$$\frac{1}{\sqrt{2\pi}} V_2(\mathbf{k}_g, \mathbf{k}_s, \omega) = \int V_1(\mathbf{k}_g, \mathbf{r}_2; \omega) d\mathbf{r}_2 \cdot \int \int dk \frac{e^{iq|z_2+z_3|}}{2iq} e^{ik(x_2-x_3)} V_1(\mathbf{r}_3, \mathbf{k}_s; \omega) d\mathbf{r}_3. \quad (67)$$

Using the convention

$$V_1(\mathbf{k}_1, -\mathbf{k}_2; \omega) \equiv \frac{1}{2\pi} \int e^{-i\mathbf{k}_1 \cdot \mathbf{r}_1} V_1(\mathbf{r}_1, \mathbf{r}_2; \omega) e^{i\mathbf{k}_2 \cdot \mathbf{r}_2} d\mathbf{r}_1 d\mathbf{r}_2$$

where  $\mathbf{k}_1 \equiv \mathbf{k}_{\text{out}} = (k_g, -q_g)$  and  $\mathbf{k}_2 \equiv \mathbf{k}_{\text{in}} = (k_s, q_s)$ . The portion of  $\mathbf{V}_2$  due to  $G_0^{\text{FS}}$  has the form

$$\sqrt{2\pi} \int dk \frac{1}{2iq} V_1(k_g, -q_g, k, q, \omega) V_1(k, -q, k_s, q_s, \omega) = V_2^{\text{FS}}(k_g, -q_g, k_s, q_s, \omega) \quad (68)$$

where  $\mathbf{k}' \equiv \mathbf{k}_{\text{out}}$  and  $\mathbf{k} \equiv \mathbf{k}_{\text{in}}$  (figure 11).

The portion of  $\mathbf{V}_2$  due only to  $G_0^{\text{FS}}$ ,  $\mathbf{V}_2^{\text{FS}}$ , is computable with  $V_1(\mathbf{k}_g, \mathbf{k}_s; \omega)$  where  $|\mathbf{k}_g| = |\mathbf{k}_s| = \omega/c_0$ , which is directly related to  $\tilde{D}$  without assumptions concerning the relationship between  $\mathbf{V}_1$  and relative changes in earth material properties. It is that portion of the inverse series that forms the free-surface demultiple subseries. Therefore, the free-surface demultiple algorithm is independent of the earth model type for the class of models we are considering. The class of models are those for which the general form,  $V(\mathbf{k}, \mathbf{k}', \omega)$ , is sufficient to describe the perturbation in the wavenumber, temporal frequency domain, and includes all elastic and certain anelastic models. If portions with  $|\mathbf{k}'| \neq \omega/c_0$  were required, then a model type constraint to compute those components would be required—this is not the case.

A summary of the free-surface demultiple algorithm (from [5, 14]) is as follows:

- (1) The data,  $D$ , are computed by subtracting the reference field,  $G_0 = G_0^d + G_0^{\text{FS}}$ , from the total field,  $G$ , on the measurement surface.

- (2) Compute the deghosted data,  $\tilde{D}$  where  $\tilde{D} = D / [(e^{2iq_g \epsilon_g} - 1)(e^{2iq_s \epsilon_s} - 1)]$ , from  $D$  and the source and receiver deghosting factors in the  $k$ - $\omega$  domain,  $G_0^d / G_0 = 1 / (e^{2iq\epsilon} - 1)$ .  $q_s$ ,  $q_g$  and  $\epsilon_s$ ,  $\epsilon_g$  are the vertical wavenumbers and the depths below the free surface of the source and receiver, respectively.
- (3) The series for deghosted and free-surface demultiplied data,  $D'$ , is given in terms of the deghosted data  $D'_1$  as follows:

$$D'_n(k_g, k_s, \omega) = \frac{1}{i\pi\rho_0 B(\omega)} \int_{-\infty}^{\infty} dk q e^{iq(\epsilon_g + \epsilon_s)} D'_1(k_g, k, \omega) D'_{n-1}(k, k_s, \omega),$$

$$n = 2, 3, 4, \dots, \quad (69)$$

and

$$D'(k_g, k_s, \omega) = \sum_{n=1}^{\infty} D'_n(k_g, k_s, \omega) \quad (70)$$

where  $D'(k_g, k_s, \omega) \equiv D'(k_g, \epsilon_g, k_s, \epsilon_s, \omega)$ ,  $B(\omega)$  and  $\rho_0$  are the source signature and reference density, respectively. The data  $D'$  consist of deghosted primaries and internal multiples only and  $D'_1 = \tilde{D}$ . Hence,  $D'$  represents the deghosted data without free-surface multiples. The mathematical details of (69) and (70) follow from (11')–(13') and are provided in [14] and [5]. Equations (69) and (70) are the prestack multi-dimensional generalizations of the one dimensional, normal incidence free-surface-elimination map presented in the appendix of [26].

A rigorous integral equation formulation relating data with free surface events to data without those events is derived by Fokkema and van den Berg [27]. A series expansion solution of the latter integral equation agrees exactly with the inverse scattering free-surface multiple removal subseries represented by (69) and (70). A feedback loop method for free-surface multiple removal was also described by Berkhout [28]. The differences between the inverse subseries for free-surface multiple removal and the feedback method are discussed in the section on data examples.

## 6. Internal multiple attenuation

### 6.1. The subseries that attenuates internal multiples

In the previous section, we described how to achieve the goal of separating the removal of surface multiples from the other three tasks of inversion. We now address the more difficult issue of separating the task of attenuating internal multiples from the last two goals of migration and inversion of primaries.

When we separated surface multiples from the other three goals we were able to isolate a portion of the Green function,  $G_0$ , namely  $G_0^{\text{FS}}$ , whose purpose in the forward and inverse series was to produce and remove, respectively, events due to the presence of the free surface. Unfortunately, for internal multiples, we do not have that relatively straightforward road to follow.

If we attempt to repeat the reasoning that proved useful with surface multiples, we seek an example that has neither free-surface *nor* internal multiples. We can imagine a problem where we have two half-spaces; that is, we wish to invert a model that has only a single horizontal reflector. In that case, the scattered field, the primary, requires for its description a complete forward scattering series in terms of  $\mathbf{G}_0^d$  and the exact perturbation,  $\mathbf{V}$ . The inverse series for  $\mathbf{V}$  in terms of the data, the primary, requires the full series and  $\mathbf{G}_0^d$ . The lesson, from this single reflector example, is that the complete  $\mathbf{G}_0^d$  is required in the inverse series when the only tasks

are locating reflectors and estimating parameters. Hence, we *cannot* separate  $\mathbf{G}_0^d$  into an extra part that exists only in the presence of internal multiples, but which is not present when internal multiples are absent. Thus, a fundamentally different approach is required for the attenuation of internal multiples.

We next present the logical path that leads to this new approach. The forward series generates primaries and internal multiples through the action of  $\mathbf{G}_0^d$  on  $\mathbf{V}$ . The inverse series constructs  $\mathbf{V}$  from the action of  $\mathbf{G}_0^d$  on the recorded data. The action of  $\mathbf{G}_0^d$  on data must remove internal multiples on the way to constructing  $\mathbf{V}$ . In an earlier section, we presented an analysis and interpretation of the forward series and, specifically, how  $\mathbf{G}_0^d$  generates primaries and internal multiples of a given order. However, before we focus on the internal multiple issue, it is important to note an essential difference between the scattering theory pictures of free-surface and internal multiple generation.

Given data,  $D'$ , without free-surface events, the forward series generates data,  $D$ , with free-surface events by the action of  $\mathbf{G}_0^{\text{FS}}$  on  $D'$ . Each term in that series generates one order of free-surface multiple—that is, all events that have reflected from the free surface a given number of times. The modelling that  $\mathbf{G}_0^{\text{FS}}$  provides is an exact description of a wave propagating in the water and reflecting from the free surface. Hence,  $\mathbf{G}_0^{\text{FS}}$  generates in the forward series and removes in the inverse series one order of free-surface multiple with each term.

The situation for primaries and internal multiples is quite different. For those events, we adopt a point-scatterer model, and every term in that forward series contributes to (but does not by itself fully describe) either primary or internal multiples. Each primary or internal multiple requires an infinite series for its construction. We adopt the simpler surface reflection model when describing wave phenomena associated with reflectors at or above the measurement surface; we adopt the point-scatterer model for waves associated with subreceiver/source structure. The former is our model of choice when we have accurate or nearly accurate information about velocities and structure and the latter is our model when that information is unavailable or unreliable.

The location and properties of the free surface are captured in  $\mathbf{G}_0^{\text{FS}}$  and it is that specific and well-defined free surface reflection experience (or its absence) which allows free-surface multiples to be separated from primaries and internal multiples with one term creating (in the forward series) and one term removing (in the inverse series) all events that have experienced the free surface a given number of times. The number of  $\mathbf{G}_0^{\text{FS}}$  factors in a term in the subseries (12'), (13') corresponds to the order of free-surface multiples that it removes. The internal multiples have (by definition) all of their downward reflections below the free surface and since we assume absolutely no subsurface information those reflectors are assumed to be completely unknown in both location and character.

This makes the problem of distinguishing the generation (and removal) of internal multiples from primaries more difficult in terms of direct propagation through water,  $\mathbf{G}_0^d$ , and the difference between earth and water properties,  $\mathbf{V}$ . As mentioned earlier, a series is required to generate any primary or any internal multiple in terms of  $\mathbf{G}_0^d$  and  $\mathbf{V}$  and new concepts are required to distinguish the forward subseries for constructing primaries from the subseries for internal multiples and then to conjecture on how to separate the tasks that act on these events in the inverse series.

It is no surprise that the first term in the forward series that constructs and first term in the inverse series that eliminates internal multiples of a given order are approximate. The efficiency of the first term in the removal subseries of internal multiples is remarkably higher than the first term in the forward creation; e.g., it takes an infinite series to get the important time prediction (phase) of any internal multiple in the forward series (in terms of  $\mathbf{G}_0^d$  and  $\mathbf{V}$ ) whereas, as we will demonstrate, the first term in the removal series (of an internal multiple

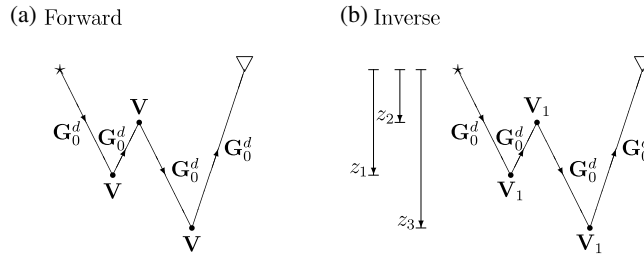


**Figure 12.** The leading term contribution to the generation of first order internal multiples is represented in (a) and suggests the leading term contribution, in the inverse series, to the removal of first order internal multiples represented in (b).  $G_0^d$ ,  $V$  and  $V_1$  are the whole-space Green function, the perturbation operator and the ‘migrated data-like’ first order approximation to  $V$ , respectively.

of a given order) predicts the time precisely and approximates well the amplitude (in terms of  $G_0^d$  and  $D'$ ) of all multiples of that order—from all reflectors at all depths at once. The efficiency of the first term of the inverse subseries for internal multiple elimination accounts for its practical value and impact.

The fact that generating primaries and internal multiples of a given order requires an infinite series suggests that an infinite series of terms, each involving operations with  $G_0^d$  on  $D'$ , is required to remove internal multiples of a given order. The particular inverse scattering subseries for attenuating all internal multiples, described here, chooses only the leading and most significant contribution from the removal series of each order of multiple, forming a series that attenuates well, rather than eliminates, all internal multiples.

In our earlier discussion of the forward series for primaries and internal multiples we argued that primaries are constructed starting with the first term in the series and that first order internal multiples have their leading contribution in the third term. Similarly, second order internal multiples are generated by contributions starting with the fifth term in the forward series. In general,  $n$ th order internal multiples have contributions from all terms starting at term  $2n + 1$ . In addition, the portion of the third term that starts to build the first order internal multiple was distinguished from the part that has a third order contribution to constructing primaries. The leading term contribution to constructing a class of multiples in the forward series suggests the leading term contribution for their removal in the inverse series (figure 12).

The first two terms in the forward series do not contribute to generating first order internal multiples. Similarly, it is argued that the first two terms in the inverse series do not contribute to their removal. The mathematical realization of figure 12(a) is the leading contribution to the generation of first order internal multiples; it suggests the corresponding mathematical expression for the leading order attenuation of those multiples. To realize, or algorithmically capture the physics associated with figure 12(b), select the portion of the third term of the inverse series with  $z_1 > z_2$  and  $z_3 > z_2$ .

With this purpose in mind we examine  $V_3$ , the third term in the inverse series. In contrast with the subseries generated by  $G_0^{FS}$ , for free-surface multiple attenuation (13'), the three terms in  $V_3$  do not sum to a single term when the inverse series is generated with the direct propagating Green function,  $G_0^d$ . From the fact that  $G_0^{FS}$  can be viewed as the Green function due to an image source above the free surface and is therefore *outside* the volume, it follows that for all  $z, z'$  inside the volume (i.e., below the free surface)  $G_0^{FS}$  satisfies the homogeneous differential equation

$$\left(\frac{\nabla^2}{\rho_0} + \frac{\omega^2}{K_0}\right)G_0^{FS} = 0.$$

The fact that  $G_0^{\text{FS}}$  satisfies a homogeneous differential equation leads in turn to the mathematical simplification

$$\begin{aligned} (\mathbf{G}_0^{\text{d}} \mathbf{V}_1 \mathbf{G}_0^{\text{FS}} \mathbf{V}_1 \mathbf{G}_0^{\text{FS}} \mathbf{V}_1 \mathbf{G}_0^{\text{d}})_m &= -(\mathbf{G}_0^{\text{d}} \mathbf{V}_1 \mathbf{G}_0^{\text{FS}} \mathbf{V}_2 \mathbf{G}_0^{\text{d}})_m \\ &= -(\mathbf{G}_0^{\text{d}} \mathbf{V}_2 \mathbf{G}_0^{\text{FS}} \mathbf{V}_1 \mathbf{G}_0^{\text{d}})_m. \end{aligned} \quad (71)$$

In computing (71),  $\mathbf{G}_0^{\text{FS}}$  does not require an off-shell  $\mathbf{k} \neq \mathbf{k}'$  contribution since its effective source (the image source) is, by definition, outside the volume supporting  $V_1$  and  $V_2$  and, hence, outside the integrals that compute terms in that particular subseries. This gives another way to understand why the free-surface demultiple algorithm is automatically model type independent. Model type was needed by Razavy [12] to provide  $T_1(k, p)$  for  $k \neq p$ . Since  $\mathbf{G}_0^{\text{FS}}$  never requires  $k \neq p$  in its integrations with  $V_1$ , it does not depend upon the inverse series model type argument to generate this subseries. Hence the free-surface multiple removal subseries is independent of the earth model type. In contrast,  $G_0^{\text{d}}$  satisfies the inhomogeneous differential equation

$$\left( \frac{\nabla^2}{\rho_0} + \frac{\omega^2}{K_0} \right) G_0^{\text{d}} = -\delta(z - z') \delta(x - x').$$

From (13'') and using  $\mathbf{G}_0^{\text{d}}$ , we have:

$$\begin{aligned} (\mathbf{G}_0^{\text{d}} \mathbf{V}_3 \mathbf{G}_0^{\text{d}}) &= -(\mathbf{G}_0^{\text{d}} \mathbf{V}_1 \mathbf{G}_0^{\text{d}} \mathbf{V}_2 \mathbf{G}_0^{\text{d}}) - (\mathbf{G}_0^{\text{d}} \mathbf{V}_2 \mathbf{G}_0^{\text{d}} \mathbf{V}_1 \mathbf{G}_0^{\text{d}}) - (\mathbf{G}_0^{\text{d}} \mathbf{V}_1 \mathbf{G}_0^{\text{d}} \mathbf{V}_1 \mathbf{G}_0^{\text{d}} \mathbf{V}_1 \mathbf{G}_0^{\text{d}}) \\ &= (\mathbf{G}_0^{\text{d}} \mathbf{V}_{31} \mathbf{G}_0^{\text{d}}) + (\mathbf{G}_0^{\text{d}} \mathbf{V}_{32} \mathbf{G}_0^{\text{d}}) + (\mathbf{G}_0^{\text{d}} \mathbf{V}_{33} \mathbf{G}_0^{\text{d}}), \end{aligned} \quad (72)$$

where

$$\mathbf{V}_{31} \equiv -\mathbf{V}_1 \mathbf{G}_0^{\text{d}} \mathbf{V}_2, \quad (73)$$

$$\mathbf{V}_{32} \equiv -\mathbf{V}_2 \mathbf{G}_0^{\text{d}} \mathbf{V}_1, \quad (74)$$

and

$$\mathbf{V}_{33} \equiv -\mathbf{V}_1 \mathbf{G}_0^{\text{d}} \mathbf{V}_1 \mathbf{G}_0^{\text{d}} \mathbf{V}_1. \quad (75)$$

In contrast to the case for  $\mathbf{G}_0^{\text{FS}}$ , these three terms  $\mathbf{V}_{31}$ ,  $\mathbf{V}_{32}$  and  $\mathbf{V}_{33}$  make distinct contributions. The first two terms,  $(\mathbf{G}_0^{\text{d}} \mathbf{V}_{31} \mathbf{G}_0^{\text{d}})$  and  $(\mathbf{G}_0^{\text{d}} \mathbf{V}_{32} \mathbf{G}_0^{\text{d}})$ , in the right member can be shown [29] to always contain a refraction-like (i.e., not reflection-like) scattering component and are thus not involved with the task of removing internal multiples. We define a reflection-like scattering (or inverse scattering) as one that changes its propagation direction with respect to the measurement surface after the interaction with  $\mathbf{V}$  (or  $\mathbf{V}_1$ ). Refraction-like scattering contributions in  $\mathbf{V}_3$  contribute to the other inversion tasks (migration and inversion) that act on primaries. The third term on the right-hand side,

$$(\mathbf{G}_0^{\text{d}} \mathbf{V}_{33} \mathbf{G}_0^{\text{d}}) = -(\mathbf{G}_0^{\text{d}} \mathbf{V}_1 \mathbf{G}_0^{\text{d}} \mathbf{V}_1 \mathbf{G}_0^{\text{d}} \mathbf{V}_1 \mathbf{G}_0^{\text{d}}),$$

can be broken up into four parts corresponding to the four diagrams in figure 13.

Choose the portion of  $(\mathbf{G}_0^{\text{d}} \mathbf{V}_{33} \mathbf{G}_0^{\text{d}})_m$  corresponding to figure 13(d); a diagram that represents a contribution to multiple *reflection* attenuation.  $(\mathbf{G}_0^{\text{d}} \mathbf{V}_{31} \mathbf{G}_0^{\text{d}})_m$  and  $(\mathbf{G}_0^{\text{d}} \mathbf{V}_{32} \mathbf{G}_0^{\text{d}})_m$  do not support a diagram of the figure 13(d) variety and therefore were not selected for that task. The mathematical and algorithmic realizations of figure 13(d) take place on requiring a lower-higher-lower relationship between the successive vertical locations of the data in the integral. Using this criterion, the appropriate portion of each of the odd terms in the series is selected. The generalization of the diagram found in figure 13(d) is used to select the appropriate portion of the leading order contribution to removing higher order internal multiples.



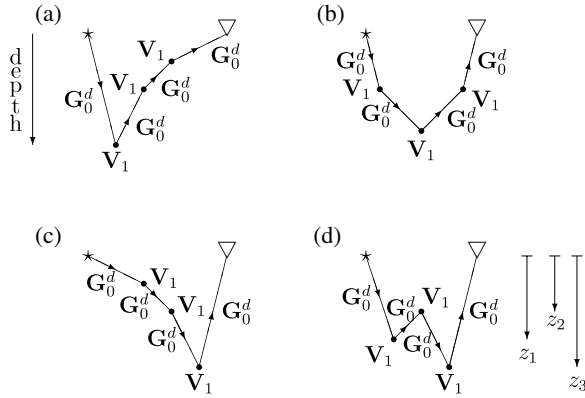


**Figure 13.** Diagrams corresponding to different portions of  $\Lambda_s G_0^d V_1 G_0^d V_1 G_0^d V_1 G_0^d \Lambda_g$ . Only (d), with  $z_1 > z_2$  and  $z_2 < z_3$ , contributes to the attenuation of first order internal multiples (see also figure 12(b)).

6.2. Internal multiple attenuation and model type dependence

For the direct propagating Green function,  $G_0^d$ , we have from (64)

$$-\frac{e^{iq|z_2-z_3|}}{2iq} = -\frac{1}{2\pi} \int_{-\infty}^{\infty} \frac{e^{iq'(z_2-z_3)}}{q^2 - q'^2 + i\epsilon} dq'$$

and separating the integral into a principal value and a contribution from contours around the poles  $q' = \pm q$  we obtain

$$\begin{aligned} \frac{1}{q^2 - q'^2 + i\epsilon} &= \text{PV} \left( \frac{1}{q^2 - q'^2} \right) + i\pi \delta(q'^2 - q^2) \\ &= \text{PV} \left( \frac{1}{q^2 - q'^2} \right) + \frac{1}{2\pi} \left( i\pi \frac{1}{2|q|} (\delta(q' - q) + \delta(q' + q)) e^{iq'(z_2-z_3)} \right). \end{aligned}$$

This contour around the pole contribution leads to

$$\int_{-\infty}^{\infty} dk \left[ \frac{V_1(k_g, -q_g, k, q) V_1(k, q, k_s, q_s)}{2iq} + \frac{V_1(k_g, -q_g, k, -q) V_1(k, -q, k_s, q_s)}{2iq} \right]$$

and is computable directly from  $V_1(k_g, q_g, k_s, q_s)$ .

The portion of  $V_2$  that depends on the principal value part of the contribution to  $G_0^d$  is not computable from  $\Psi_s(x_g, \epsilon_g, x_s, \epsilon_s, \omega)$  without assuming a model type; hence it was excluded from the computation. Since the internal multiple algorithm derives from the analogous  $i\pi \delta$  contributions from the  $V_1 V_1 V_1$  or  $V_{33}$  (see (75)) contribution from the third term in the series (equation (13'')),

$$\int dk dk' \left[ \frac{V_1(k_g, -q_g, k, q) V_1(k, q, k', -q') V_1(k', -q', k_s, q_s)}{(2iq)(2iq')} + \dots \right]$$

is once again computable directly from surface data without assumption of model type.

An important point to recognize in deriving the internal multiple algorithm, not emphasized in previous publications, is that although the ‘W’ or lower–higher–lower relationship from the forward series provides a guide for the examination of a similar diagram in the inverse, to actually realize an internal multiple algorithm, the quantity taken through the diagram was not

$\mathbf{V}_1$  but rather  $b_1$ : the effective data generated by a single frequency plane-wave incident field given by

$$b_1(k_g, \epsilon_g, k_s, \epsilon_s, q_g + q_s) = (-2iq_s)D'(k_g, \epsilon_g, k_s, \epsilon_s, \omega) = \frac{V_1(k_g, q_g, k_s, q_s, \omega)}{-2iq_g}.$$

This was originally deduced through empirical evaluation and testing of different candidate quantities (e.g. a first and natural guess of taking  $\mathbf{V}_1$  through ‘W’ does not lead to an attenuation algorithm) that, in turn, allow different subdivisions of the  $\mathbf{V}_{33}$  term in terms of a ‘W’ diagram [5, 29].

The fact that  $b_1$  results in localized incident and scattered (reflected) wavefronts in every dimension (without the wake behind the wavefront in the 1D and 2D impulse response represented by  $D'$ ) is the only and best understanding or hint we have for this fact to date. That is, it seemed that the internal multiple attenuation algorithm favoured a quantity to be taken through the ‘W’ diagram that in every dimension would correspond to a scattered field with all spike-like or localized events. Neither  $\mathbf{V}_1$  nor  $D'$  satisfies that criterion in every dimension, but  $-2iq_s D'$  does. Hence, the forward construction and inverse removal ‘W’ diagram symmetry for the internal multiple went only so far and the fact that  $b_1$  is the quantity that when transformed to  $(k_g, q_g, z)$  and broken into lower–higher–lower contributions results in the internal multiple algorithm remains partly intuitive and empirical in its foundation and invites further physical interpretation and mathematical analysis. A deeper comprehension of the workings of the inverse series will also benefit the current research on imaging and inverting primaries.

The internal multiple attenuation algorithm operates in a 1D, 2D or 3D earth and is independent of the model type because it derives from an algorithm depending on the portion of  $\mathbf{V}_1$  and  $\mathbf{V}_3$  that only requires  $|\mathbf{k}_g| = |\mathbf{k}_s| = \omega/c_0$ .

The inverse scattering series is not computable for a general operator of the form  $\mathbf{V}(\mathbf{p}, \mathbf{k}, \omega)$  where the vectors  $\mathbf{p}$  and  $\mathbf{k}$  have the same dimension as the subsurface, e.g., they are three dimensional vectors for a three dimensional earth, but are otherwise independent of each other and  $\omega$ . However, the subseries of the inverse series for  $\mathbf{V}(\mathbf{p}, \mathbf{k}, \omega)$  that results from only the  $i\pi\delta$  contributions, where  $|\mathbf{p}| = |\mathbf{k}| = \omega/c_0$ , is directly computable without assuming a model type. When seeking model type-independent algorithms (as is the case for the free-surface demultiple algorithm), you either demonstrate that the principal value contribution is zero, or in the case of the internal multiple attenuation algorithm you choose from the beginning only the portion of the inverse series to task subdivide that is independent of model type. A model type-independent task-specific subseries provides a selection criterion for seeking and isolating certain terms and ignoring others.

We anticipate that the refraction-like inverse-scattering contributions that play a role in imaging primaries at depth and progressing from internal multiple attenuation to elimination will be model type independent when either the measured wavefield contains both reflection and transmission data (e.g., surface reflection and vertical seismic profiles) or when transmission data can be constructed from reflection data. The fourth task, that of earth mechanical properties identification, will certainly require specification of what set of parameters you seek to identify and will therefore be model-type specific. That three of the four tasks associated with inversion would be model-type independent speaks to the conceptual and practical value of that approach and strategy.

### 6.3. Internal multiple attenuation algorithm

The first term in the internal multiple attenuation subseries is the data,  $D'$ , consisting of primaries and internal multiples. The second term in this series comes from a portion of the

third term in the inverse series ((72) and (75)). This portion of the third term,

$$\begin{aligned}
 b_3(k_g, k_s, q_g + q_s) &= \frac{1}{(2\pi)^2} \int_{-\infty}^{\infty} \int_{-\infty}^{\infty} dk_1 e^{-iq_1(\epsilon_g - \epsilon_s)} dk_2 e^{iq_2(\epsilon_g - \epsilon_s)} \\
 &\times \int_{-\infty}^{\infty} dz_1 e^{i(q_g + q_1)z_1} b_1(k_g, k_1, z_1) \int_{-\infty}^{z_1} dz_2 e^{i(-q_1 - q_2)z_2} b_1(k_1, k_2, z_2) \\
 &\times \int_{z_2}^{\infty} dz_3 e^{i(q_2 + q_s)z_3} b_1(k_2, k_s, z_3), \tag{76}
 \end{aligned}$$

is chosen to satisfy  $z_1 > z_2$  and  $z_2 < z_3$ .  $b_1$  is defined in terms of the original prestack data with free-surface multiples eliminated,  $D'$ , and is defined by

$$D'(k_g, k_s, \omega) = (-2iq_s)^{-1} B(\omega) b_1(k_g, k_s, q_g + q_s) \tag{77}$$

where  $B(\omega)$  is the source signature and, once again,  $b_1$  represents the data that would result from a single frequency incident plane wave. The data with internal multiples attenuated,  $D^{\text{IM}}$ , are

$$D^{\text{IM}}(k_g, k_s, \omega) = (-2iq_s)^{-1} B(\omega) \sum_{n=0}^{\infty} b_{2n+1}(k_g, k_s, q_g + q_s) \tag{78}$$

where  $D^{\text{IM}}$  contains the primaries with their wavelet. A recursive relationship that generalizes (78) and provides  $b_{2n+1}$  in terms of  $b_{2n-1}$  for  $n = 1, 2, 3, \dots$  is given in [29] as

$$\begin{aligned}
 b_{2n+1}(k_g, k_s, q_g + q_s) &= \frac{1}{(2\pi)^{2n}} \int_{-\infty}^{\infty} dk_1 e^{-iq_1(\epsilon_g - \epsilon_s)} \\
 &\times \int_{-\infty}^{\infty} dz_1 e^{i(q_g + q_1)z_1} b_1(k_g, k_1, z_1) A_{2n+1}(k_1, k_s, z_1), \\
 n &= 1, 2, 3, \dots, \tag{79}
 \end{aligned}$$

where

$$\begin{aligned}
 A_3(k_1, k_s, z_1) &= \int_{-\infty}^{\infty} dk_2 e^{iq_2(\epsilon_g - \epsilon_s)} \int_{-\infty}^{z_1} dz_2 e^{i(-q_1 - q_2)z_2} b_1(k_1, k_2, z_2) \\
 &\times \int_{z_2}^{\infty} dz_3 e^{i(q_2 + q_s)z_3} b_1(k_2, k_s, z_3)
 \end{aligned}$$

and

$$\begin{aligned}
 A_{2n+1}(k_1, k_s, z_1) &= \int_{-\infty}^{\infty} dk_2 e^{iq_2(\epsilon_g - \epsilon_s)} \int_{-\infty}^{z_1} dz_2 e^{i(-q_1 - q_2)z_2} b_1(k_1, k_2, z_2) \\
 &\times \int_{-\infty}^{\infty} dk_3 e^{-iq_3(\epsilon_g - \epsilon_s)} \int_{z_2}^{\infty} dz_3 e^{i(q_2 + q_3)z_3} \\
 &\times b_1(k_2, k_3, z_3) A_{2n-1}(k_3, k_s, z_3), \quad n = 2, 3, 4, \dots
 \end{aligned}$$

As we mentioned, the full series for  $\mathbf{V}$  can have restrictive convergence properties (see, e.g., [14]). In contrast, numerical tests indicate that the internal multiple attenuation subseries in (79) always converges and is insensitive to missing low frequency information [29–31].

Free-surface multiple attenuation methods operate one temporal frequency at a time (see (69) and (70)); in contrast, the attenuation of an internal multiple from a single frequency of data requires data at all frequencies (see (78) and (79)). This requirement derives from the integral over temporal frequency in the transform of  $q_g + q_s$  to  $z$ . With band-limited data this transform is only approximate; nevertheless, the truncated integral remains effective at attenuating multiples. As in the case of the free-surface multiple removal algorithm, each term

in the series in (78) attenuates a given order of internal multiple and prepares the higher order internal multiples for the higher order demultiple terms in the series. Since  $e^{ik_z z} b_1(k_g, k_s, \omega)$  is a downward continuation of shots and receivers to depth  $z$  in the reference medium and subsequent integration over  $k_z$  is a simple constant Jacobian away from integration over  $\omega$  ( $t = 0$  imaging condition), it follows that  $b_1(k_g, k_s, z)$  corresponds to uncollapsed migration [3, 32]. Indeed, the algorithm can be interpreted as a sequence of these uncollapsed migrations restricted to lower–higher–lower pseudo-depths.

Pseudo-depth and migration are terms often used in exploration geophysics. Pseudo-depth refers to the location of an image derived using the background reference velocity. Since the reference velocity is constant (water), pseudo-depth is essentially vertical travel time. Migration refers to the imaging process where subsurface reflectors are ‘migrated’ from the incorrect to the correct location. Uncollapsed migration is a generalization of the original migration concept; sources and receivers are downward continued to a common depth level  $z$ , time is evaluated at zero and information at  $x_g \neq x_s$  is retained. The latter retention of  $x_g \neq x_s$  distinguishes uncollapsed migration from migration; it provides local angle-dependent reflection coefficients rather than the angle-averaged reflection coefficient of the traditional  $x_g = x_s$  imaging condition (see [32]).

The process of obtaining a primaries-only data set starts with  $D$ : a data set with free-surface and internal multiples and primaries.  $D$  is then input into the free-surface demultiple algorithm to produce  $D'$ , which is then used as input to the internal multiple attenuation algorithm to output data that contain primaries.

## 7. Analytic, numerical and field data examples of free-surface and internal multiple attenuation

### 7.1. Purposeful perturbation

As we have described, the combination of the apparent lack of robust convergence of the entire inverse series, without a level of *a priori* information that is generally not achievable, and the recognition that it nevertheless represented the only complete inversion formalism for multi-dimensional acoustic and elastic waves motivated the search for task-specific subseries that would have more favourable properties. At the same time, another issue that these task-specific and well-converging subseries faced was how many terms would be required in practice to achieve a certain level of effectiveness towards the specific task associated with that subseries. The concept of purposeful perturbation was developed to address the latter issue.

The idea is to identify the specific purpose or role that each term within a task-specific subseries performs independent of the subsurface or target over which the recorded data were collected.

The terms of the series perform uncoupled and coupled tasks; the task-specific subseries perform isolated, uncoupled tasks. We define the purposeful perturbation concept as knowledge of precisely what each term within a given task-specific subseries is designed to accomplish. For example, a term in the inverse scattering subseries for eliminating free-surface multiples removes precisely one order of free-surface multiple completely independent of the depth of the water or any other property or characteristic of the earth.

### 7.2. 1D free-surface demultiple algorithm (example of purposeful perturbation)

If the subseries that we isolate accomplishes one of the four broad tasks (described in section 2.5), then purposeful perturbation further determines and defines the specific role or

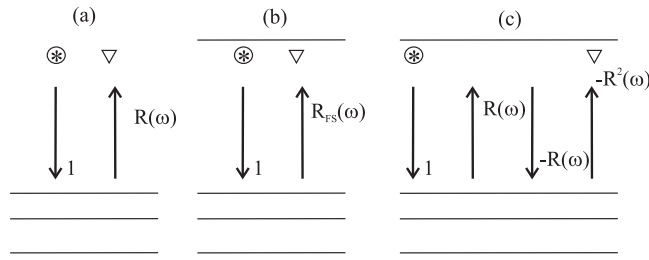


**Figure 14.** An illustration of the free-surface multiple removal series: (a) data without a free surface, (b) the total upgoing field in the presence of a free surface  $R_{FS}$  and (c) the series for  $R_{FS}$  in terms of  $R$ .

subtask that individual terms in that subseries perform in completing the overall task associated with that subseries. For example, if you estimate the range of depths of potential hydrocarbon reservoirs in a given setting and the depth to the water bottom is known, then you have a good way to determine the highest order of water bottom multiple that you need to be concerned with and precisely the number of terms in the free-surface demultiple subseries ((69) and (70)) that can accomplish that objective.

For the simplest illustration of this purposeful perturbation concept, consider the generation of free-surface multiples for a 1D earth, whose primary reflections and internal multiples have a response  $R(\omega)$ ; and, where the free surface is characterized by a reflection coefficient of  $-1$  for a pressure wavefield (see figure 14).

For source and receiver deghosted data and a source wavelet with unit amplitude, the upgoing field in the presence of a free surface  $R_{FS}$  is able to be written in terms of  $R(\omega)$  by imagining (see figure 14 (c)) the wave first leaving the source moving down into the earth; that incident unit pressure wave generates a reflected response from the earth,  $R(\omega)$ , consisting of primaries and internal multiples. This in turn propagates as a train up through the water column until it hits the free surface, where it experiences a  $-1$  reflection coefficient and heads down through the water columns as  $-R(\omega)$  and is incident upon the earth as a long ‘wavelet’. The impulse response of the earth  $R(\omega)$  times this effective downgoing ‘wavelet’,  $-R(\omega)$ , produces a new wave moving up from the earth through the water column towards the free surface. This process continues and results in the total upgoing wave in the presence of the free surface,  $R_{FS}(\omega)$ , in terms of the primary and internal multiple wavefield,  $R(\omega)$ , as follows:

$$\begin{aligned}
 R_{FS} &= R - R^2 + R^3 - \dots \\
 &= \frac{R}{1 + R}.
 \end{aligned}
 \tag{80}$$

Each term in (80) generates all free-surface multiples of a given order independent of any detail of the subsurface. The order of a free-surface multiple corresponds to the number of times that event has experienced a reflection at the free surface. Since each successive term in (80) comes from one additional reflection at the free surface, it generates one additional order of free-surface multiple. If you were interested in creating free-surface multiples up to a given order, then understanding the purpose of each term in (80) allows you to know precisely how many terms that objective would require. Solving (80) for the data without free-surface multiples,  $R$ , we have

$$\begin{aligned}
 R &= \frac{R_{FS}}{1 - R_{FS}} \\
 &= R_{FS} + R_{FS}^2 + R_{FS}^3 + \dots
 \end{aligned}
 \tag{81}$$

The first term in (81),  $R_{\text{FS}}$ , is the upgoing portion of the reflection data that contains all primaries, internal multiples and free-surface multiples. When the second term,  $R_{\text{FS}}^2$ , is added to  $R_{\text{FS}}$  two things happen: (1) all free-surface multiples that have reflected once (and only once) from the free surface are removed and (2) all higher order free-surface multiples are altered in preparation for higher terms, e.g.,  $R_{\text{FS}}^3$ , to remove them order by order, as well. This well-defined action of the terms in the free-surface demultiple series is totally independent of any water bottom or subsurface detail (of course, within an assumed 1D, 2D or 3D dimension of the earth variation).

This is an example of purposeful perturbation; and it has enormous practical significance. For example, if you estimate that for a given depth of water and target, only a certain order of multiples could be troublesome, then you know precisely how many terms in the series you need to use in your processing algorithm for that data. Equation (81) is the 1D normal incidence special case of the general multi-dimensional inverse scattering subseries for free-surface multiple removal (69) and (70) (see also [5, 14]).

Equation (81) is the 1D antecedent of (11') to (13'), (69) and (70) for free-surface multiple removal. Several observations about equations (80) and (81) are worth noting. First, the role of  $\mathbf{G}_0^{\text{FS}}$ , the extra portion of  $\mathbf{G}_0$  due to the free surface is played by the  $(-1)$  reflection coefficient in deriving (80) and its inverse (81). Second, the forward construction series was a guide (and in this simple instance, more than a guide) to the inverse process. Only the free-surface reflection coefficient  $(-1)$  terms enter (i.e.,  $\mathbf{G}_0^{\text{FS}}$ ) confirming the forward and removal series (80) and (81), respectively. Focusing on only this single task, we see that no coupled terms in  $\mathbf{G}_0^{\text{FS}}$ ,  $\mathbf{G}_0^{\text{d}}$  appear in the analogous and transparently simple (80) and (81), which is consistent with, and supports, the strategy that we described for the generalized algorithm that derives from the multi-dimensional inverse series.

Regarding some practical issues, if instead of a unit incident pulse a wavelet  $A(\omega)$  was the source signature, then (80) would become

$$R_{\text{FS}} = \frac{A(\omega)R}{1 + R} \quad (82)$$

and (81) becomes

$$R = \frac{\frac{R_{\text{FS}}}{A(\omega)}}{1 - \frac{R_{\text{FS}}}{A(\omega)}} = \frac{R_{\text{FS}}}{A(\omega)} + \left( \frac{R_{\text{FS}}}{A(\omega)} \right)^2 + \dots \quad (83)$$

and, hence, the wavelet is a critical requirement for the free-surface multiple removal and all subseries application (see, e.g., [33–35]).

A similar process of purposeful perturbation occurs (and has been identified) for the internal multiple removal series. Understanding the specific purpose of each term within an overall task reveals what has (and has not) been achieved for a given finite number of terms providing a critically important practical guide for field data application as well as mitigating issues of overall convergence and rate of convergence.

### 7.3. 1D analytic example of the internal multiple attenuation algorithm

The 2D internal multiple algorithm is described in (76)–(79). The first term in this series is

$$b(k_g, k_s, q_g + q_s) = -2iq_s D'(k_g, k_s, \omega)$$

where  $D'$  represents the data resulting from an impulsive source and after free-surface multiple removal. The second term in this series is  $b_3$ , given by

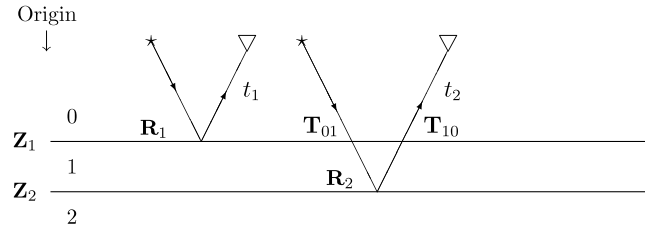


Figure 15. A one dimensional model with two interfaces.

$$\begin{aligned}
 b_3(k_g, k_s, q_g + q_s) &= \frac{1}{(2\pi)^2} \int_{-\infty}^{\infty} \int_{-\infty}^{\infty} dk_1 e^{iq_1(\epsilon_s - \epsilon_g)} dk_2 e^{iq_2(\epsilon_g - \epsilon_s)} \\
 &\times \int_{-\infty}^{\infty} dz_1 e^{i(q_g + q_1)z_1} b_1(k_g, -k_1, z_1) \int_{-\infty}^{z_1} dz_2 e^{i(-q_1 - q_2)z_2} b_1(k_1, -k_2, z_2) \\
 &\times \int_{z_2}^{\infty} dz_3 e^{i(q_2 + q_s)z_3} b_1(k_2, -k_s, z_3).
 \end{aligned}$$

The first two terms in the internal multiple attenuation series attenuate all first order internal multiples. For a 1D earth and a normal incidence plane wave, (76) reduces to

$$b_3(k) = \int_{-\infty}^{\infty} dz_1 e^{ikz_1} b(z_1) \int_{-\infty}^{z_1} dz_2 e^{-ikz_2} b(z_2) \int_{z_2}^{\infty} dz_3 e^{ikz_3} b(z_3). \quad (84)$$

To explicitly demonstrate how the internal multiple attenuation algorithm works and to examine its properties, we will consider the simplest model that can produce an internal multiple. For the model shown in figure 15 the reflection data due to an impulsive incident wave  $\delta(t - \frac{z}{c})$  are

$$D'(t) = R_1 \delta(t - t_1) + T_{01} R_2 T_{10} \delta(t - t_2) + \dots$$

where  $t_1, t_2, R_1, R_2$  are the two way times and reflection coefficients from the two reflectors and  $T_{01}$  and  $T_{10}$  are the coefficients of transmission between model layers 0 and 1 and 1 and 0, respectively;

$$D'(\omega) = R_1 e^{i\omega t_1} + T_{01} R_2 T_{10} e^{i\omega t_2} + \dots \quad (85)$$

where  $D'(\omega)$  is the temporal Fourier transform of  $D'(t)$ .

Note that the  $(-2iq_s)$  factor that multiplies  $D'$  in the internal multiple theory is not required in this example since we assume that the incident wave is an impulsive plane wave. The role of  $(-2iq_s)$  is to transform an incident (or reference field)  $\mathbf{G}_0$  into a plane wave in the Fourier domain. The input into the internal multiple algorithm is  $b$ : data with primaries and internal multiples. This is also the first term in the multiple attenuation series, thus  $b_1 = b$  and

$$b^{\text{IM}}(k) = b_1(k) + b_3(k) + b_5(k) + \dots$$

The vertical wavenumber is

$$k_z = \sqrt{(\omega/c_0)^2 - k_{x_g}^2} + \sqrt{(\omega/c_0)^2 - k_{x_s}^2}$$

and for a 1D medium and a normal incident wave it is  $k_z = 2\frac{\omega}{c_0}$  and

$$b(k_z) = D(\omega). \quad (86)$$

The reflection data from (85) and (86) are expressed in terms of  $k_z$ :

$$b(k_z) = R_1 \exp\left(i\left(\frac{2\omega}{c_0}\right)\left(\frac{c_0 t_1}{2}\right)\right) + T_{01} R_2 T_{10} \exp\left(i\left(\frac{2\omega}{c_0}\right)\left(\frac{c_0 t_2}{2}\right)\right) + \dots \quad (87)$$

and define the pseudo-depths  $z_1$  and  $z_2$  in the reference medium as

$$z_1 \equiv \frac{c_0 t_1}{2},$$

$$z_2 \equiv \frac{c_0 t_2}{2}.$$

The input data are now expressed in terms of  $k = k_z$  and  $z_1$  and  $z_2$  as

$$b(k) = R_1 e^{ikz_1} + T_{01} R_2 T_{10} e^{ikz_2} + \dots \quad (88)$$

ready for the internal multiple algorithm.

Substitute the data from (88) into the algorithm in (84). After transforming from  $k = k_z$  to  $z$ ,

$$b(z) = \int_{-\infty}^{\infty} e^{-ikz} b(k) dk. \quad (89)$$

The first integral in (84) towards computing  $b_3$  is

$$\int_{z'_2 + \epsilon_1}^{\infty} dz'_3 e^{ikz'_3} (R_1 \delta(z'_3 - z_1) + R'_2 \delta(z'_3 - z_2) + \dots) \quad (90)$$

where

$$R'_2 \equiv T_{01} R_2 T_{10}$$

where  $\epsilon_1$  is a small positive parameter chosen to ensure that the ‘W’ diagram is strictly lower–higher–lower and avoids the lower than or equal to contribution. In actual seismic field data application the parameter  $\epsilon$  is chosen to be the width of the source wavelet and attests to the fact that subresolution (i.e., thin bed multiples) will not be attenuated. The integral (90) evaluates to

$$H(z_1 - (z'_2 + \epsilon_1)) R_1 e^{ikz_1} + H(z_2 - (z'_2 + \epsilon_1)) R'_2 e^{ikz_2}$$

where  $H$  is the Heaviside or step function.

The second integral in (84) is

$$\begin{aligned} & \int_{-\infty}^{z'_1 - \epsilon_2} (R_1 \delta(z'_2 - z_1) + R'_2 \delta(z'_2 - z_2)) (H(z_1 - (z'_2 + \epsilon_1)) R_1 e^{ikz_1} \\ & \quad + H(z_2 - (z'_2 + \epsilon_1)) R'_2 e^{ikz_2}) e^{-ikz'_2} dz'_2 \\ & = R_1^2 H((z'_1 - \epsilon_2) - z_1) \underline{H(z_1 - (z_1 + \epsilon_1))} e^{ikz_1} e^{-ikz_1} \\ & \quad + R_1 R'_2 H((z'_1 - \epsilon_2) - z_2) \underline{H(z_1 - (z_2 + \epsilon_1))} e^{ikz_1} e^{-ikz_2} \\ & \quad + R_1 R'_2 H((z'_1 - \epsilon_2) - z_1) H(z_2 - (z_1 + \epsilon_1)) e^{ikz_2} e^{-ikz_1} \\ & \quad + (R'_2)^2 H((z'_1 - \epsilon_2) - z_2) \underline{H(z_2 - (z_2 + \epsilon_1))} e^{ikz_2} e^{-ikz_2} \end{aligned} \quad (91)$$

where  $\epsilon_2$  is a positive parameter with the same purpose as  $\epsilon_1$  and all the underlined terms are zero.

The third and last integral is

$$\begin{aligned} b_3(k) & = \int_{-\infty}^{\infty} dz'_1 e^{-ikz'_1} (R_1 \delta(z'_1 - z_1) + R'_2 \delta(z'_1 - z_2)) \\ & \quad \times (R_1 R'_2 H((z'_1 - \epsilon_2) - z_1) H(z_2 - (z_1 + \epsilon_1)) e^{ikz_2} e^{-ikz_1}) \\ & = e^{ikz_1} R_1^2 R'_2 \underline{H(-\epsilon_2)} H(z_2 - z_1 + \epsilon_1) e^{ikz_2} e^{-ikz_1} \\ & \quad + e^{ikz_2} R_1 (R'_2)^2 H(z_2 - z_1 - \epsilon_2) H(z_2 - z_1 - \epsilon_1) e^{ikz_2} e^{-ikz_1} \end{aligned}$$

and the underlined term is zero.



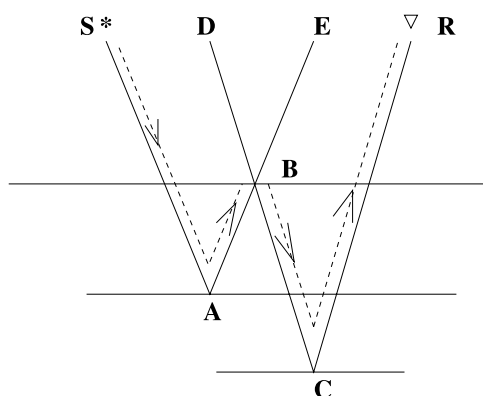


Figure 16. Subevents for an internal multiple.

Since

$$R'_2 = T_{01} R_2 T_{10},$$

the prediction is

$$b_3(k) = R_1 R_2^2 T_{01}^2 T_{10}^2 e^{2ikz_2} e^{2ikz_2} e^{-ikz_1}$$

and

$$b_3(t) = R_1 R_2^2 T_{01}^2 T_{10}^2 \delta(t - (2t_2 - t_1)).$$

From the example it is easy to compute the actual first order internal multiple precisely:

$$-R_1 R_2^2 T_{01} T_{10} \delta(t - (2t_2 - t_1)).$$

Hence the prediction of time is perfect and the amplitude of the prediction has an extra power of  $T_{01} T_{10}$ , thus defining exactly the difference between the attenuation represented by  $b_3$  and elimination. Since  $T_{01} T_{10}$  is less than one, the method will always attenuate internal multiples. Furthermore, the residual after adding  $b_1$  to  $b_3$  has the same sign as the multiple. Hence, the internal multiple algorithm has well-defined amplitude prediction properties. If  $R_1 = 1/4$  (a large reflection coefficient) then  $T_{01} T_{10} = 15/16$ . Therefore even with large  $R_1$ ,  $T_{01} T_{10}$  is still not far from 1 which explains the remarkable efficiency of the leading order term for removing first order multiples. It produces the precise timing of all internal multiples of first order, independent of where the upward and downward reflections occur and approximates well their amplitudes (always less than the actual); the precise relationship between the internal multiple amplitude and the  $b_3$  prediction is quantified. Since the difference in amplitude is related to transmission information, the internal multiple predictor could also provide indirect but potentially useful overburden transmission estimates. Hence, while it is accurate to say that the internal multiple attenuation algorithm does not predict the exact amplitude, it is not accurate to say that no significant useful amplitude information is predicted by the internal multiple attenuation algorithm. In fact, for internal multiples of entirely P-wave histories, their amplitudes are typically reduced by 80–95%. Further terms beyond the first in the internal multiple elimination subseries would result in an algorithm that eliminates rather than attenuates internal multiples.

A diagrammatic example also serves to illustrate how the timing of internal multiples is predicted. In figure 16 we show an internal multiple (dashed line), SABCR. Primaries SABE, DBCR and DBE have a phase relationship with the internal multiple SABCR such that

$$(SABE)_{\text{time}} + (DBCR)_{\text{time}} - (DBE)_{\text{time}} = (SABCR)_{\text{time}}.$$

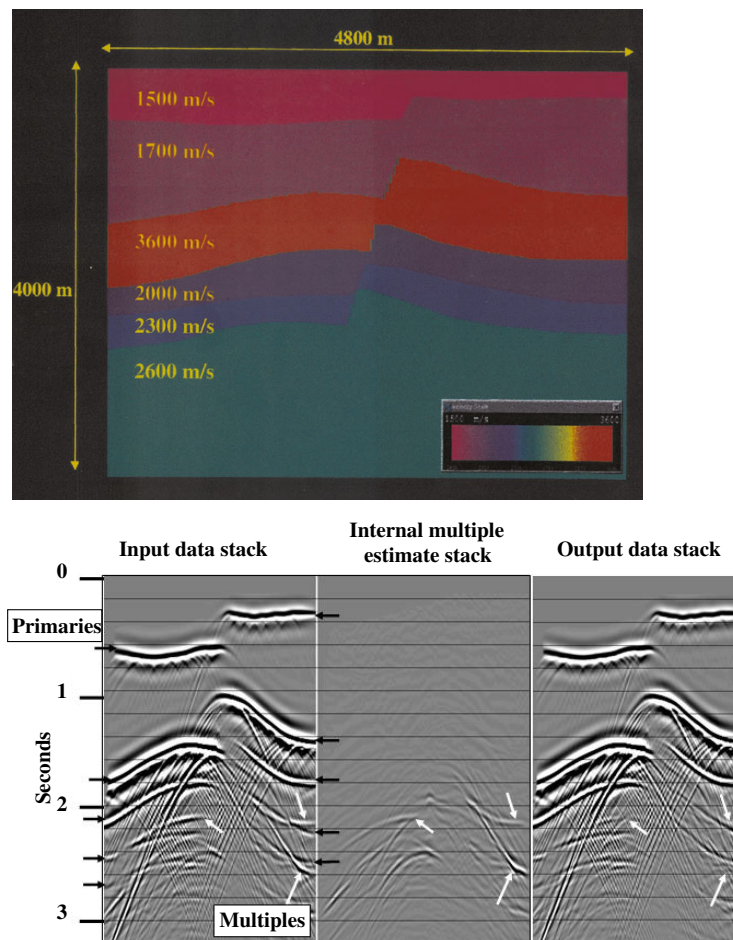


**Figure 17.** A 2D synthetic model (top). The left panel (bottom) shows a common offset display from the synthetic data set created using the model. The middle panel (bottom) shows the predicted internal multiples and the right-hand panel (bottom) is the result after subtracting the predicted multiples from the input data set.

Hence, if the overall data contain three events such that two are longer time events and if the sum of the time of the two longer events *minus* one smaller time event corresponds to the time of the event under investigation, the event is an internal multiple and, if so, it is removed. The algorithm also predicts well the amplitude and thus can distinguish between a multiple and a temporally coincident primary at any given offset. This is the reason the third term in the inverse series, that involves three  $D(t)$  data terms, starts the process of internal multiple removal and why the 'W' diagram (see figure (16)) is at the heart of the internal multiple prediction from the data procedure; and, finally, why the time prediction of all internal multiples is accurate. The signs of the phases in the three exponentials in (76) are consistent with this timing relationship.

#### 7.4. Synthetic and field data examples

Figure 17 shows an example of the internal multiple attenuation series algorithm applied to a 2D synthetic data set. From left to right, the three panels show the input data, the predicted internal multiples and the result of inverse scattering internal multiple attenuation, respectively.

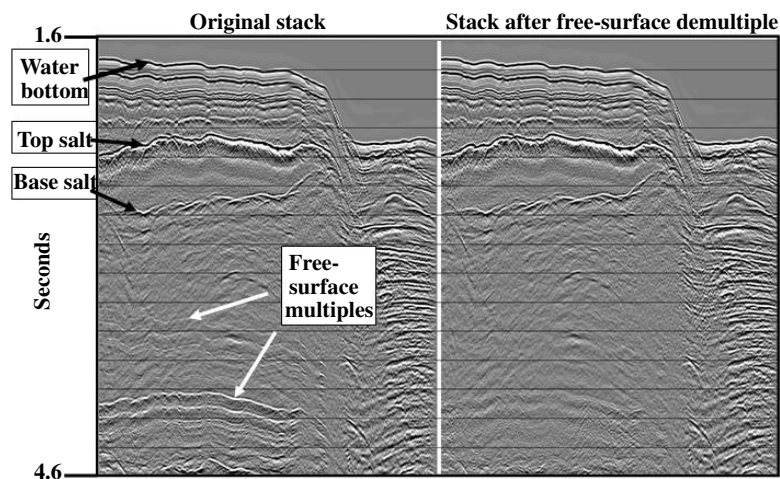


**Figure 18.** The left panel is a stack of a field data set from the Gulf of Mexico. The right panel is the result of inverse-scattering free-surface multiple removal. Data are courtesy of WesternGeco.

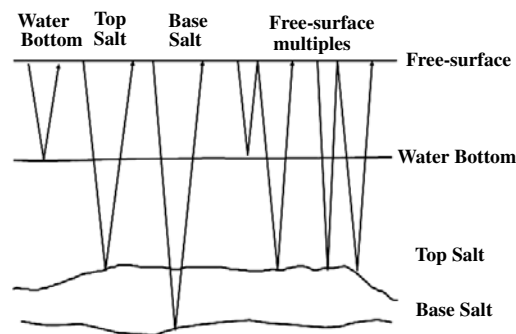


**Figure 19.** A cartoon illustrating the events that are used by the algorithm to predict free-surface multiples.

Figures 18–20 illustrate the free-surface and internal multiple attenuation algorithms applied to a data set from the Gulf of Mexico over a complex salt body. Seismic imaging beneath salt is a challenging problem due to the complexity of the resultant wavefield. In figure 18, the left panel is a stacked section of the input data and the right panel shows the result of the inverse scattering free-surface multiple removal algorithm. Figure 19 is a cartoon that illustrates the events that are used by the algorithm to predict the free-surface multiples in the data. Figure 20 illustrates the internal multiple attenuation method applied to the same Gulf of Mexico data set. An internal multiple that has reverberated between the top of the salt body and the water bottom is well attenuated through this method. The cartoon in figure 21 illustrates the subevents that are used by the algorithm to predict the internal multiples.

A number of practical prerequisites need to be satisfied to realize successful results on field data. First, the spatial sampling of the data needs to be done with sufficient aperture and density to ensure accuracy of the multiple predictions. Missing near offsets (the source–receiver distance) are often a problem encountered in normal data acquisition and these offsets need to be estimated or extrapolated. Current marine acquisition design collects mainly a narrow azimuth of data. Hence, this limits the application of the demultiple algorithms to 2D.

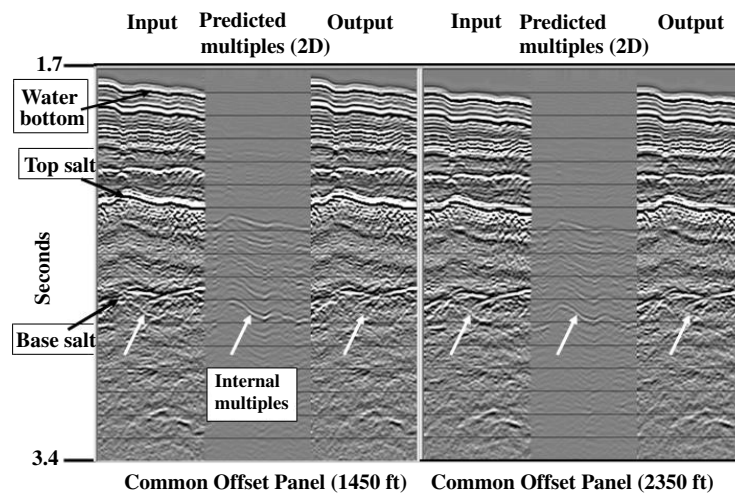


**Figure 20.** An example of inverse-scattering internal multiple attenuation from the Gulf of Mexico. Data are courtesy of WesternGeco.

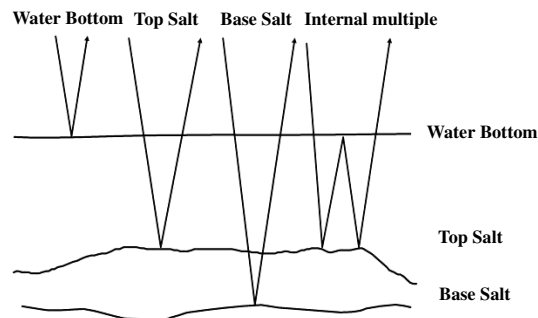


**Figure 21.** A cartoon illustrating the events that are used by the algorithm to predict a subsalt internal multiple.

A more complete sampling of the wavefield enables full 3D implementation of these algorithms. Presentations at recent international exploration meetings indicate that several oil and service companies are currently performing full 3D application of free-surface multiple removal.

Another key practical issue is obtaining an accurate estimate of the source time function or source wavelet. A wide suite of methods for estimating this wavelet exist. The wavelet estimation method in common use today for multiple attenuation seeks to turn the algorithm's very need for the wavelet into its own indicator that the criterion is satisfied. This strategy requires that a distinguishing property of reflection data with multiples compared to data without multiples is first identified. Then the wavelet is sought such that after applying the demultiple algorithm, the condition of multiple-free data is satisfied. The current realization of that thinking begins by arguing that data without multiples have fewer events than data with multiples and hence less energy; therefore, seek the wavelet that produces a minimal energy for the multiple attenuation output. A 1D energy criterion was introduced and different single term approaches [33, 35] and multiple term global search algorithms [36] were developed. An overview of current approaches to that issue is presented by Matson [37]. In some way, the 1D

energy minimization methods for finding the wavelet represent a weak link in how free-surface and internal multiple attenuation is applied in practice. The methods for finding the wavelet are not as physically complete (and effective) as the multiple removal methods that they are meant to serve. For example, the free-surface and internal multiple attenuation methods have no problem with interfering events; but the removal of a multiple proximal to and destructively interfering with a primary could cause the energy to rise (rather than fall) with the removal of the multiple. New methods (e.g., [38–41]) are being developed for predicting the wavelet that are as complete as, and on a conceptual and effectiveness par with, the inverse series multiple attenuation procedures that they are meant to serve.

Often the series is truncated to only a single multiple prediction term and an adaptive wavelet estimation scheme is used to adaptively subtract the internal multiples from the input data. For internal multiples, numerical tests indicate that it is more difficult to estimate the wavelet post-internal multiple prediction. This is due to the fact that the 1D minimum energy criterion is often invalid and too blunt an instrument for the subtlety of internal multiples and complex free-surface multiples. Fortunately, the two processes require the same wavelet; thus the wavelet estimated for the free-surface multiple attenuation step will often suffice for internal multiple attenuation, as was the case in the field data example shown here. Currently, compromises made with truncated series algorithms, too great a dependence on adaptive parameters and less than adequate measurement coverage are all inhibiting the full power of these methods from being realized. With multi-term series applications, improved predicted wavelets and a full 3D point receiver acquisition, we anticipate that the inverse scattering demultiple methods will reach their full practical potential.

### *7.5. Inverse scattering series and the feedback methods for attenuating multiples*

Removing multiples from seismic reflection data is a long-standing problem that has experienced significant progress over the past ten years, but still has open issues to address. An overview of the landscape of techniques can be found in [42] and several collaborative works with members of the Delphi group (e.g., [43, 44]). Berkhout, Verschuur and the Delphi group developed a free-surface and interface feedback procedure for describing free-surface multiples and primaries and internal multiples and also for attenuating free-surface and internal multiples, respectively. The inverse scattering approach uses the free surface for free-surface multiples and a point-scatterer model for primaries and internal multiples. The inverse-scattering free surface demultiple method is conceptually complete, whereas the free-surface feedback approach represents certain compromises that involve the obliquity factor and source deghosting that place an added burden on the adaptive wavelet, especially at large distances from the source along the receiver line. The feedback method provides an effective and efficient method for attenuating internal multiples when the reflector that generates the downward reflection can be isolated. The inverse scattering series approach provides the most comprehensive method for attenuating all free-surface and internal multiples with no subsurface information whatsoever and no event picking, velocity analysis or interpretive intervention.

The inverse scattering series methods provide significant added value when the subsurface is complex, when reflectors are dipping, corrugated or diffractive, when events are subtle and partly coincident in time and when the interest is in removing all internal multiples. Issues that involve the practical prerequisites of these series solutions are all important and methods for satisfying those prerequisites include source signature estimation, areal coverage of surface measurements and deghosting. Considerable resources are currently devoted to addressing and improving the satisfaction of these prerequisites.

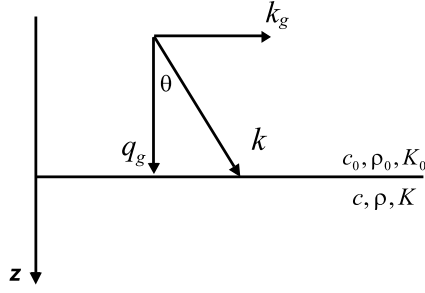


Figure 22. The relationship between  $q_g$ ,  $k_g$  and  $\theta$ .

### 8. Inverse subseries for imaging and inversion at depth without an accurate velocity model for large contrast complex targets

Initial analysis for identifying the imaging and inversion tasks associated with primaries within the series has recently been reported by Weglein *et al* [45]. Starting with the acoustic equation (6) and defining

$$\begin{aligned}\frac{1}{K} &= \frac{1}{K_0}(1 + \alpha), \\ \frac{1}{\rho} &= \frac{1}{\rho_0}(1 + \beta)\end{aligned}$$

for a one dimensional variable velocity and density acoustic medium with point sources and receivers at depth  $\epsilon_s$  and  $\epsilon_g$ , respectively, (11'') becomes

$$\tilde{D}(q_g, \theta, \epsilon_g, \epsilon_s) = -\frac{\rho_0}{4} e^{-iq_g(\epsilon_s + \epsilon_g)} \left[ \frac{1}{\cos^2 \theta} \tilde{\alpha}_1(-2q_g) + (1 - \tan^2 \theta) \tilde{\beta}_1(-2q_g) \right] \quad (92)$$

where the subscripts s and g denote source and receiver respectively and  $q_g$ ,  $\theta$  and  $k = \omega/c_0$  are shown in figure 22 and have the following relations:

$$\begin{aligned}q_g &= q_s = k \cos \theta, \\ k_g &= k_s = k \sin \theta.\end{aligned}$$

Similarly the solution for  $\alpha_2(z)$  and  $\beta_2(z)$  as a function of  $\alpha_1(z)$  and  $\beta_1(z)$  can be obtained from (12'') as

$$\begin{aligned}\frac{1}{\cos^2 \theta} \alpha_2(z) + (1 - \tan^2 \theta) \beta_2(z) &= -\frac{1}{2 \cos^4 \theta} \alpha_1^2(z) - \frac{1}{2} (1 + \tan^4 \theta) \beta_1^2(z) \\ &+ \frac{\tan^2 \theta}{\cos^2 \theta} \alpha_1(z) \beta_1(z) - \frac{1}{2 \cos^4 \theta} \alpha_1'(z) \int_0^z dz' [\alpha_1(z') - \beta_1(z')] \\ &+ \frac{1}{2} (\tan^4 \theta - 1) \beta_1'(z) \int_0^z dz' [\alpha_1(z') - \beta_1(z')].\end{aligned} \quad (93)$$

For a single reflection between two acoustic half-spaces where the upper half-space corresponds to the reference medium the data consist of primaries only and the inversion tasks they face are simply locating the reflector and inverting for acoustic property changes across the reflector. When the primary data from this two half-space model are substituted into (92) and (93), then the two terms involving integrals on the right-hand side become zero. If the model allowed a second reflector and two primary wavefields, then those same terms involving the integrals would not be zero. From an inversion point of view, the primary from

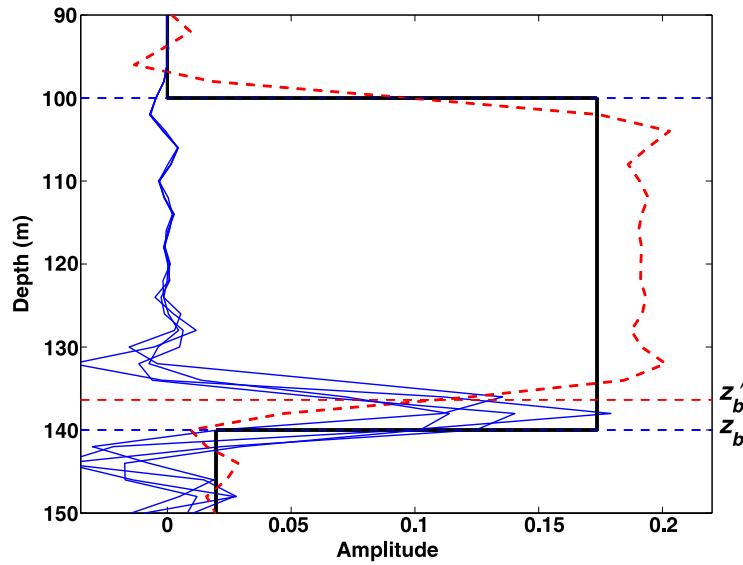


**Figure 23.** Five terms in the leading order imaging subseries. The solid black curve shows the actual perturbation  $\alpha$  and the dashed red curve shows  $\alpha_1$ , the first approximation to  $\alpha$ . The blue curves show the leading order imaging subseries terms. The cumulative sum of these imaging terms is shown in figure 24.

the second reflector has more required inversion tasks to perform (in comparison with the first primary), since the first event actually travelled through the reference medium. In addition to estimating changes in earth material properties, the second primary will be imaged where it is placed by the reference medium. From this type of observation and the detailed analysis in [45] and [46], it is deduced that the last two terms in (93) assist in moving the second (deeper) primary to its correct location and the first three terms of (93) are associated with improving the linear inversion in (92), including mitigating the effect of not having removed the influence of transmission through the shallower reflector on the deeper reflector and the subsequent non-linear inversion of the deeper primary.

The terms on the right-hand side of (93) have two objectives. For a primary from the shallower reflector, the first objective is to start the non-linear process of turning the reflection coefficient of that event into the earth property changes  $\alpha$  and  $\beta$ . The reflection coefficient is a non-linear series in  $\alpha$  and  $\beta$ ; and, conversely,  $\alpha$  and  $\beta$  are themselves non-linear series in the reflection coefficient. For the simple horizontal reflector between two elastic half-spaces, that forward non-linear relationship is expressed by the Zoeppritz equations (see [47]). Methods for inverting that relationship are either linear direct or based on non-linear indirect (modelling) with global search matching engines [48]. The inverse series represents the only multi-dimensional direct non-linear inversion for medium properties without iteration or assumptions about the dimension or geometry of the target. For the second (deeper) primary, the first objective is more complicated, since the event amplitude is a function of both the reflection coefficient at the second reflector and the transmission coefficient downward through and upward past the first reflector. This first objective is accomplished by the first three terms on the right-hand side of (93). The communication between the two events allowed in, e.g.,  $\alpha_1^2$  can be shown to allow the reflection coefficient of the shallower reflector to work towards removing the transmission coefficients impeding the amplitude of the second event from inverting for

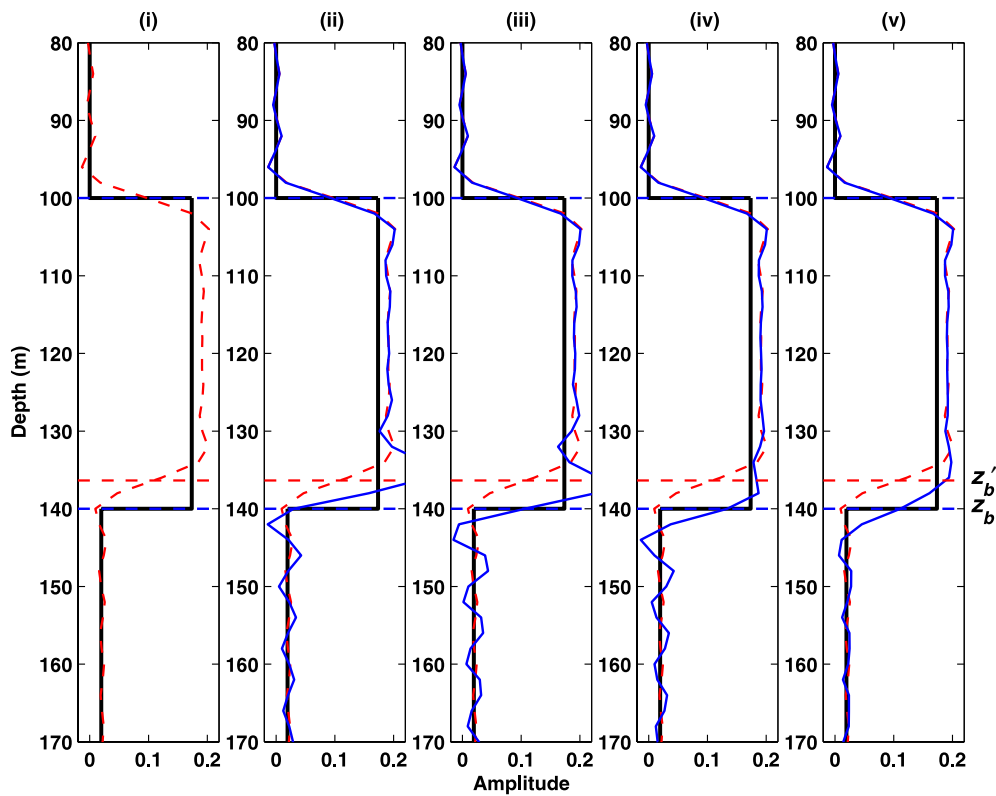


**Figure 24.** The cumulative sum of five terms in the leading order imaging subseries. The solid black curve shows the perturbation  $\alpha$  and the red curve shows the first approximation to  $\alpha$  or the first term in the inverse series,  $\alpha_1$ . The blue curve shows the cumulative sum of the imaging subseries terms; e.g. in panel (ii) the sum of two terms in the subseries is shown and in panel (v) the sum of five terms in the subseries is displayed.

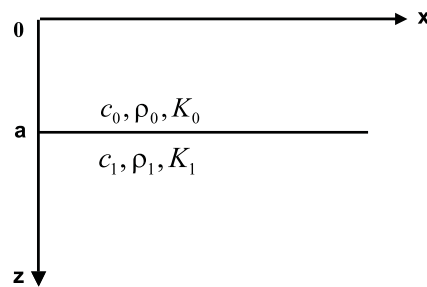


**Figure 25.** A one dimensional acoustic model.

local properties at the second reflector. Hence, specific communications between primaries from different reflectors work together to remove the extraneous transmission coefficients on deeper primaries that are suffering from being given the wrong imaging velocity.

Similarly, the integral terms on the right-hand side of (93) represent a recognition that the reference velocity will give an erroneous image and asks for an integral of  $\alpha_1 - \beta_1$ , the linear approximation to the change in acoustic velocity, from the onset of  $\alpha_1 - \beta_1$  down to the depth



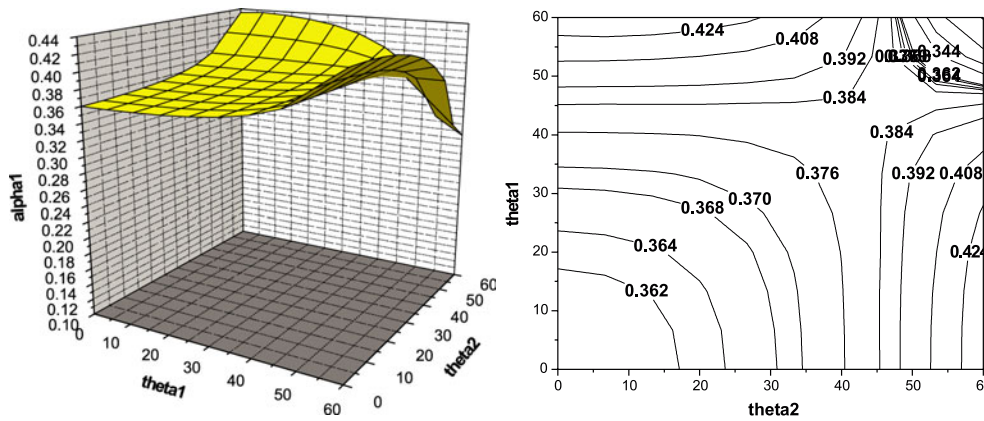


Figure 26.  $\alpha_1$  displayed as a function of two angles. The graph on the right is a contour plot of the graph on the left. In this example, the exact value of  $\alpha$  is 0.292.

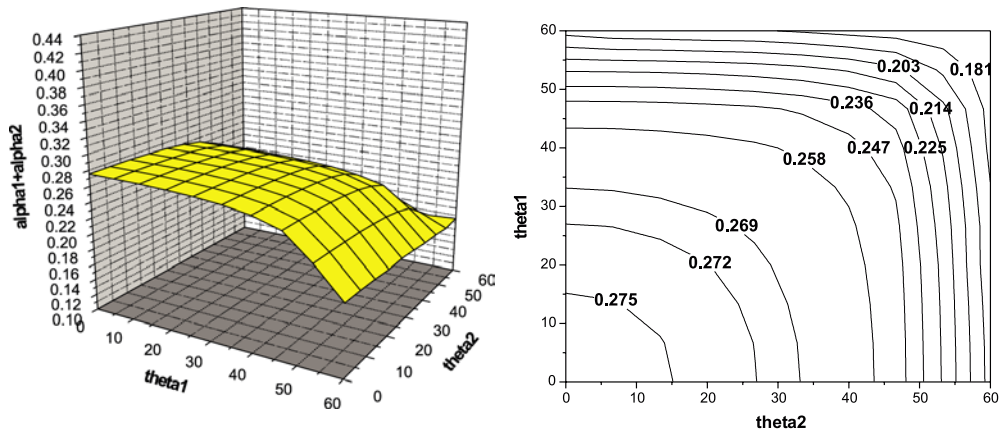
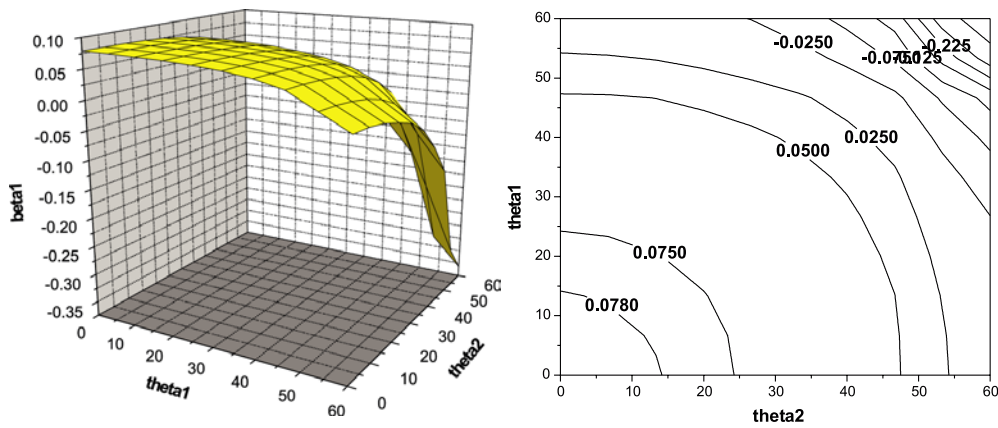


Figure 27. The sum  $\alpha_1 + \alpha_2$  displayed as a function of two angles for the same example as in figure 26 where the exact value of  $\alpha$  is 0.292.

needing the imaging help. Two important observations. (1) When the actual velocity does not change across an interface,  $R(\theta)$  is not a function of  $\theta$  and from (92) it can be shown that

$$\alpha_1 - \beta_1 = \left( \frac{\Delta V}{V} \right)_1 = 0.$$

Therefore, when the actual velocity does not change then the linear approximation to the change in velocity is zero. Therefore, when the velocity is equal to the reference across all reflectors (e.g., when density changes but not velocity) then these equations do not correct the location where the reference velocity locates those events, which in that case is correct. (2) The error in locating reflectors caused by an error in velocity depends on both the size of the error and the duration of the error. Hence, the integral of  $\alpha_1 - \beta_1$  represents an amplitude and duration correction to the originally mislocated primary. A general principle is that when an inversion task has a duration aspect for the problem being addressed, the response has an integral over a measure of that error in the solution. The inverse series empowers the primary events in the data to ‘speak to themselves’ for non-linear inversion and to ‘speak to each other’ to deal with



**Figure 28.**  $\beta_1$  displayed as a function of two angles. The graph on the right is a contour plot of the graph on the left. In this example, the exact value of  $\beta$  is 0.09.

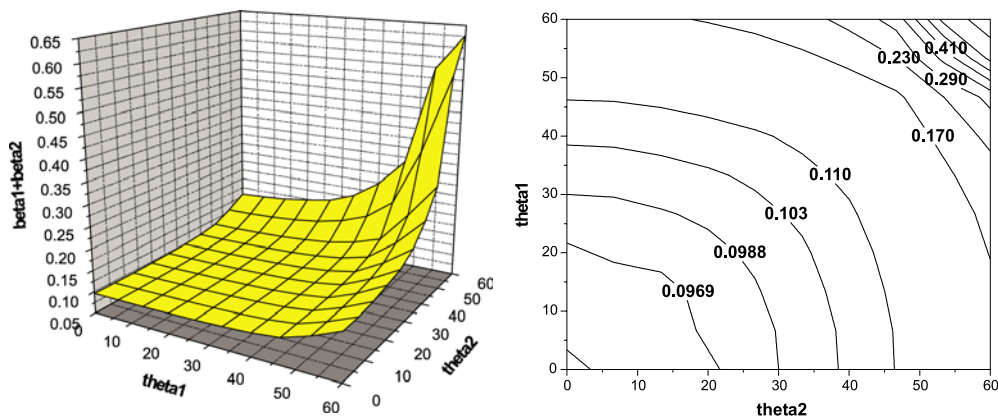


**Figure 29.** The sum  $\beta_1 + \beta_2$  displayed as a function of two angles for the same example as in figure 28 where the exact value of  $\beta$  is 0.09.

the effect of erroneous velocity on amplitude analysis for either location or inversion tasks. The analogous ‘discussion between events’ for multiple removal is described in the conclusions.

Figures 23 and 24 illustrate the imaging portion of the inverse series for a 1D constant density, variable velocity acoustic medium. The depth to which the reference velocity images the second reflector is  $z_{b'} = 136$  m. The band-limited singular functions of the imaging subseries act to extend the interface from  $z_{b'}$  to  $z_b$  (figure 23). The cumulative sum of these imaging subseries terms is illustrated in figure 24. After summing five terms the imaging subseries has converged and the deeper reflector has moved towards its correct depth  $z_b = 140$  m.

Figures 26–29 are a comparison of linear and non-linear predictions for a two parameter acoustic medium and for the 1D single interface example illustrated in figure 25. Figure 26 shows  $\alpha_1$  as a function of two different angles of incidence for a chosen set of acoustic parameters. Figure 27 shows the sum  $\alpha_1 + \alpha_2$  and demonstrates a clear improvement as an estimate for  $\alpha$ , for all precritical angles. Figure 29 illustrates similar improvements for the second parameter, the relative change in density  $\beta$ , over the linear estimate given in figure 28.

**Table 1.** Summary of task-specific subseries.

Task	Properties
Free-surface multiple elimination	One term in the subseries predicts precisely the time and amplitude of all free-surface multiples of a given order independently of the rest of the history of the event. Order is defined as number of times the multiple has a downward reflection at the free surface.
Internal multiple attenuation	One term in the inverse series predicts the precise time and approximate amplitude of all internal multiples of a given order. The order of an internal multiple is defined by the number of downward reflections from any subsurface reflector at any depth.
Imaging at depth without the accurate velocity	The first term in the series corresponds to current migration or migration-inversion. To achieve a well-estimated depth map requires further terms in the imaging subseries directly in terms of an inaccurate velocity model. <i>A priori</i> velocity estimation will aid the rate of convergence.
Inversion at depth without the exact overburden	The first term in the subseries corresponds to current linear amplitude analysis. Improvement to linear estimates of earth property changes and accounting for inadequate overburden requires further terms in the series. Tests indicate rapid convergence for the first non-linear parameter estimation objective.

Early analysis and tests are encouraging and demonstrate the intrinsic potential for the task-specific inverse subseries to perform imaging at the correct depth [49] and improving upon linear estimation of earth material properties [50], without the need for an accurate velocity model. Furthermore, numerical tests indicate: (1) that the imaging subseries converges for velocity errors that are large in amplitude and duration; and (2) rapid improvement in estimates of earth material properties beyond the current industry standard linear amplitude analysis.

## 9. Conclusions and summary

We have described the historical development and a methodology for deriving direct multi-dimensional non-linear seismic data processing methods from the inverse scattering series. To date, the inverse scattering series have yielded subseries for free-surface and internal multiple attenuation, imaging primaries at depth and inverting for earth material properties. The hallmark of these methods is their ability to achieve their objective directly in terms of incomplete or inaccurate *a priori* subsurface information and without ever iterating or updating that input or assuming that it is proximal to actual properties.

The development features an interplay between an understanding of the forward scattering process and task separation in the inverse scattering series. The forward series begins with the reference propagator,  $\mathbf{G}_0$ , and the perturbation operator,  $\mathbf{V}(\mathbf{r}, \omega)$ , the difference between actual and reference medium properties as a function of space,  $\mathbf{r}$ , and frequency  $\omega$ . The inverse series inputs data,  $D(\mathbf{r}_g, \mathbf{r}_s, t)$ , a function of time and the reference propagator,  $\mathbf{G}_0$ .

Since the forward series inputs the perturbation,  $\mathbf{V}(\mathbf{r}, \omega)$ , and rapid variation of  $\mathbf{V}$  corresponds to the exact spatial location of reflectors, it follows that space is the domain of comfort of the forward series. In contrast, the computation of the time of arrival of any (and every) seismic event for which the actual medium propagation is not described by  $\mathbf{G}_0$  requires an infinite series to obtain the correct time from the forward series. In this respect, time is the domain of discomfort for the forward series for seismic events.

For the inverse series, the input is data in time  $D(\mathbf{r}_g, \mathbf{r}_s, t)$  and processes that involve transforming  $D(\mathbf{r}_g, \mathbf{r}_s, t)$  to another function of time, e.g., the data without free-surface multiples  $D'(\mathbf{r}_g, \mathbf{r}_s, t)$ , are simpler to achieve than tasks such as imaging primaries in space that require a map from time to space (i.e.,  $D(\mathbf{r}_g, \mathbf{r}_s, t)$  to  $\mathbf{V}(\mathbf{r}, \omega)$ ). Hence, time is the domain of comfort for the inverse series. Emphasizing this point, the correct time (and amplitude) for constructing any internal multiple requires an infinite number of terms in the forward series whereas the prediction of the precise time and well-approximated amplitude for every internal multiple occurs in the first term of the inverse (removal) subseries for that order of multiple, totally independently of the depths of the reflectors that generate the multiple.

In addition, if accurate *a priori* information can be provided for the localization and separation of a given task where the task is defined in terms of separating events that have a well-defined experience from those events that have not, then further efficiency can derive from subseries that involve time to time maps, for example, in the case where a free-surface reflection coefficient (or  $\mathbf{G}_0^{\text{FS}}$ ) is supplied for the task of removing the ghosts and free-surface multiples. In the latter case, one term in the free-surface multiple removal subseries precisely predicts the time and amplitude of all multiples of that order. In table 1, we summarize the amount of effort required to achieve a certain level of effectiveness for each of the four task-specific subseries.

The strategy is to accomplish one task at a time, in the order listed, and then restart the problem as though the just completed task never existed. This is advantageous in that it avoids the terms associated with coupled tasks in the inverse series. Furthermore, carrying these tasks out in sequence can enhance the ability of subsequent tasks to reach their objective. For example, the free-surface and internal multiple algorithms do not require (or benefit from) accurate *a priori* information. However, the removal of free-surface and internal multiples significantly improves our ability to estimate the overburden velocity model and subsequently aids the efficacy and efficiency of the imaging and inversion subseries for primaries.

Since the rate of convergence, for both multiple removal subseries, does not benefit from anything closer to the earth than water speed and the costs of the algorithms quickly increase with complexity of the reference medium, the idea is to perform these tasks with efficient, constant water velocity reference propagation.

In tackling the next step, the approach is to restart the problem assuming that certain data issues have already been addressed. For example, after free-surface and internal multiple removal, we restart the problem assuming a primary-only data set resulting in an inverse series that requires proximal velocity information and consequently more complex and more costly subseries for tasks that benefit from that additional information.

If you do not like the strategy of ‘isolate a task and then restart the problem’ and you want to be a purist and start and end with one inverse scattering series, then you would need a single complex reference medium that would allow the toughest task to have an opportunity to succeed. There are two issues with the latter approach:

- (1) the proximal velocity can be difficult to obtain when troublesome multiples are in your input data; and
- (2) the single all-encompassing series is an ‘all or nothing’ strategy that does not allow for stages to succeed and provide benefit when the overall series or its more ambitious goals are beyond reach.

Although both primaries and multiples have experienced the subsurface and, hence, carry information encoded in their character, the indisputable attitude or orientation of the inverse

scattering series (the only currently known multi-dimensional direct inversion method for acoustic and elastic media) is to treat multiples as coherent noise to be removed and treat primaries as the provider of subsurface information. That does not mean that one could never use multiples in some inclusive rather than exclusive method that seeks to exploit the information that both primaries and multiples contain. It simply means that an inclusive theory, starting with realistic *a priori* information, does not currently exist and, further, that the inverse series definitely and unambiguously adopts the exclusive view: multiples are considered noise that it removes while primaries are the signal with useful subsurface information.

While it certainly follows from the mathematics of (11)–(14) that it is possible to directly achieve seemingly impossible inversion objectives from data with only a reference medium propagator that is assumed to be not equal to  $\mathbf{G}$  and hence inadequate, there is also value in providing an understanding from an information content point of view (see also [5]). What basically happens in each task-specific subseries is that specific conversations take place between events in the data as a whole that allow, e.g., multiple prediction or accurate depth imaging to take place without an accurate velocity model. ‘Non-linear in the data’ is the key and means that quadratic terms enter the picture (data times data, at least) and that allows different events to have multiplicative communication.

For example, if you provide the medium in detail you can readily determine through modelling whether any event in the data is a primary or multiple. However, if you provide only an isolated event, without the medium properties, then there is no way to determine whether it is a primary or multiple; in fact it can be either for different models. So how does the inverse series work out whether the event is a primary or multiple without any subsurface information? Since it is a series, there is a ‘conversation’ set up with other events and then a yes or no as to whether an event is a primary or multiple is completely achievable without any information about the medium.

In the subseries for imaging at depth without an accurate velocity, the first term is the current state-of-the-art migration with your best estimated velocity model and places each event exactly where that input reference velocity dictates. All current imaging methods are linear in the data, and once the velocity model is chosen, the collection of all primaries (from all reflectors) as a whole are not asked their ‘view’ or ‘opinion’ of the input velocity nor are they allowed to ‘discuss’ it amongst themselves.

The second term in the inverse series, e.g. (93), has integral terms that start to move the incorrectly imaged events resulting from the linear migration step towards their correct location. There is a quadratic dependence on the data, allowing multiplicative conversations between primary events from two different reflectors, and they are empowered to have an opinion about the input velocity. If they decide together that (at least) one of the events has been provided with a velocity model that is inconsistent with those two events, then the troubled event (usually deeper) asks for assistance from a shallower event to help it use its amplitude, and the difference of their arrival times, to move the deeper primary towards its correct location. Furthermore, and perhaps most important, when the first term beyond current best practice is computed, the quadratic term immediately and unambiguously judges the adequacy of the input velocity. If the result of the first non-linear conversation between primaries (represented by the terms with integrals in the imaging series) is a determination that the velocity is adequate, then the imaging series stops, and returns a zero value for the correction to spatial location sending the message that the data all together judge the velocity as adequate and to proceed with current linear migration for locating reflectors in space. There is no mindless (and costly) perturbation about no change in depth—rather a clear signal to stop the imaging series. This is another important example of purposeful perturbation. The term containing  $\int (\alpha_1 - \beta_1) dz$  in (93) exists to correct depth imaging for incorrect input velocity, but first determines whether

its function is required by a conversation between all the primaries about the adequacy of the velocity expressed through  $\alpha_1 - \beta_1$ . As we explained,  $\alpha_1 - \beta_1$  will be computed as zero when the velocity is adequate.

When the velocity is determined to be adequate, the inversion subseries that predicts changes in earth material properties will provide added value beyond current industry practice for arbitrary geometry of target and small or large changes in elastic properties and density across the target. When the velocity is determined to be inadequate, those same non-linear inversion objectives are achieved directly in terms of the inadequate velocity model. Hence, the inverse series and the task-specific subseries represent a fundamentally new capability for imaging and inverting primaries, as they had earlier provided for the removal of multiples.

In progressing from migration to migration-inversion [3, 32] one addressed not just where the reflector is located in space but also what material properties changed across that imaged reflector. One issue in making that step is the need to consider both the amplitude as well as the phase of the back-propagating wave in the estimated reference medium. When the ability to estimate the reference medium is far from adequate and migration-inversion is performed in the reference medium as a first step in the imaging subseries, then the bar on the migration-inversion is higher still (in comparison to migration-inversion when the reference is adequate and the latter is the final product) requiring a need for fidelity on phase, amplitude and spectral content. The imaging subseries expects the complete and correct migration-inversion in the *incorrect* medium. Since the relationships between variables and their Fourier conjugates are markedly different in, e.g., wave, coherent state and asymptotic migration techniques, we would expect a preference for wave theory migration and an appropriate sampling and coverage of surface recording that preserves, e.g., all  $k_g$  components in a given  $x_g$ .

Serious conceptual and practical hurdles in the theoretical evolution, algorithm development and robust industrial application had to be overcome to bring the inverse scattering multiple attenuation subseries methods to their current state of efficacy. We anticipate that in bringing the subseries for imaging and inverting primaries through that same process, still higher hurdles and tougher prerequisites will be addressed. This new vision of processing signal in seismic data has game-changing potential for the exploration and production of hydrocarbons. We would also anticipate that these inverse scattering series methods and the new methods for satisfying their prerequisites (e.g., source signal identification) might serve to encourage other fields of non-destructive evaluation to benefit from these efforts—fields such as medical imaging, environmental monitoring, nuclear, atomic and molecular identification and signal enhancement, military and defence detection, identification and guidance applications and global and crustal seismology.

### Acknowledgments

Craig Cooper, Jon Sheiman, Robert Keys, Michael Bostock, Roel Snieder, Kris Innanen, Fons ten Kroode, Tadeusz Ulrych and Ken Larner are thanked for useful and constructive comments and suggestions. The support of the M-OSRP sponsors is gratefully acknowledged. The Texas Advanced Research Program (ARP # 003652-0624-2001) is acknowledged for partial support of this research.

### References

- [1] Cohen J K and Bleistein N 1977 An inverse method for determining small variations in propagation speed *SIAM J. Appl. Math.* **32** 784–99
- [2] Morley L and Claerbout J 1983 Predictive deconvolution in shot-receiver space *Geophysics* **48** 515–31
- [3] Stolt R H and Weglein A B 1985 Migration and inversion of seismic data *Geophysics* **50** 2458–72

- [4] Weglein A B, Boyse W E and Anderson J E 1981 Obtaining three-dimensional velocity information directly from reflection seismic data: an inverse scattering formalism *Geophysics* **46** 1116–20
- [5] Weglein A B, Gasparotto F A, Carvalho P M and Stolt R H 1997 An inverse scattering series method for attenuating multiples in seismic reflection data *Geophysics* **62** 1975–89
- [6] Newton R G 2002 *Scattering Theory of Waves and Particles* (New York: Dover)
- [7] Taylor J R 1972 *Scattering Theory* (New York: Wiley)
- [8] Clayton R W and Stolt R H 1981 A Born–WKB inversion method for acoustic reflection data *Geophys. Soc. Explor. Geophys.* **46** 1559–67
- [9] Matson K H 1997 An inverse-scattering series method for attenuating elastic multiples from multicomponent land and ocean bottom seismic data *PhD Thesis* University of British Columbia
- [10] Moses H E 1956 Calculation of scattering potential from reflection coefficients *Phys. Rev.* **102** 559–67
- [11] Prosser R T 1969 Formal solutions of inverse scattering problems *J. Math. Phys.* **10** 1819–22
- [12] Razavy M 1975 Determination of the wave velocity in an inhomogeneous medium from reflection data *J. Acoust. Soc. Am.* **58** 956–63
- [13] Stolt R H and Jacobs B 1980 Inversion of seismic data in a laterally heterogeneous medium *SEP Rep.* **24** 135–52
- [14] Carvalho P M 1992 Free-surface multiple reflection elimination method based on nonlinear inversion of seismic data *PhD Thesis* Universidade Federal da Bahia, Brazil (in Portuguese)
- [15] ten Kroode F 2002 Prediction of internal multiples *Wave Motion* **35** 315–38
- [16] Weglein A B and Matson K 1998 Inverse-scattering interval multiple attenuation: an analytic example and subevent interpretation *Mathematical Methods in Geophysical Imaging (Proc. SPIE vol 3453)* ed S Hassanzadeh (Bellingham, WA: SPIE) pp 1008–17
- [17] Coates R T and Weglein A B 1996 Internal multiple attenuation using inverse scattering: results from prestack 1 and 2D acoustic and elastic synthetics *66th Ann. Int. SEG Mtg* pp 1522–5 (expanded abstracts)
- [18] Matson K 1996 The relationship between scattering theory and the primaries and multiples of reflection seismic data *J. Seism. Explor.* **5** 63–78
- [19] Nita B, Matson K and Weglein A B 2003 Forward scattering series seismic events: far-field approximations, critical and postcritical reflections *SIAM J. Appl. Math.* submitted
- [20] Innanen K A and Weglein A B 2003 *Viscoacoustic Born Series Continued: Toward Scattering-Based Q Compensation/Estimation* in preparation
- [21] Keys R G and Weglein A B 1983 Generalized linear inversion and the first Born theory for acoustic media *J. Math. Phys.* **24** 1444–9
- [22] Devaney A J and Weglein A B 1989 Inverse scattering using the Heitler equation *Inverse Problems* **5** L49–52
- [23] Weglein A B, Matson K H, Foster D J, Carvalho P M, Corrigan D and Shaw S A 2000 Imaging and inversion at depth without a velocity model *70th Ann. Int. SEG Mtg (Calgary, Alberta, 2000)*
- [24] Boyse W E 1986 *Wave Propagation and Inversion in Slightly Inhomogeneous Media* p 40
- [25] Boyse W E and Keller J B 1986 Inverse elastic scattering in three dimensions *J. Acoust. Soc. Am.* **79** 215–8
- [26] Ware J A and Aki K 1969 Continuous and discrete inverse-scattering problems in a stratified elastic medium. I. Plane waves at normal incidence *J. Acoust. Soc. Am.* **45** 911–21
- [27] Fokkema J T and van den Berg P M 1993 *Seismic Applications of Acoustic Reciprocity* (Amsterdam: Elsevier)
- [28] Berkhout A J 1982 *Seismic Migration, Imaging of Acoustic Wave energy by Wavefield Extrapolation, A: Theoretical Aspects* 2nd edn (Amsterdam: Elsevier)
- [29] Araújo F V 1994 Linear and nonlinear methods derived from scattering theory: backscattered tomography and internal multiple attenuation *PhD Thesis* Universidade Federal da Bahia, Brazil (in Portuguese)
- [30] Araújo F V, Weglein A B, Carvalho P M and Stolt R H 1994 Internal multiple attenuation *56th Meeting of Association of Exploration Geophysicists, session H036*
- [31] Araújo F V, Weglein A B, Carvalho P M and Stolt R H 1994 Inverse scattering series for multiple attenuation: an example with surface and internal multiples *64th Ann. Int. SEG Mtg* pp 1039–41 (expanded abstracts)
- [32] Weglein A B and Stolt R H 1999 Migration-inversion revisited *Leading Edge* **18** 950–2
- [33] Ikelle L T, Roberts G and Weglein A B 1995 Source signature estimation based on the removal of first order multiples *65th Ann. Int. SEG Mtg* pp 1478–81 (expanded abstracts)
- [34] Verschuur D J, Berkhout A J and Wapenaar C P A 1992 Adaptive surface-related multiple elimination *Geophysics* **57** 1166–77
- [35] Verschuur D J and Berkhout A J 1992 Surface-related multiple elimination and wavelet estimation *54th EAEG Mtg* vol 7, pp 568–9
- [36] Carvalho P M and Weglein A B 1994 Wavelet estimation for surface multiple attenuation using a simulated annealing algorithm *64th Ann. Int. SEG Mtg (Los Angeles, CA, 1994)* (expanded abstracts)

- [37] Matson K H 2000 An overview of wavelet estimation using free-surface multiple removal *Leading Edge* **19** 50–5
- [38] Weglein A B and Secrest B G 1990 Wavelet estimation from marine pressure measurements *Geophysics* **63** 2108–19
- [39] Osen A, Secrest B G, Amundsen L and Reitan A 1998 Wavelet estimation from marine pressure measurements *Geophysics* **63** 2108–19
- [40] Tan T H 1999 Wavelet spectrum estimation *Geophysics* **64** 1836–46
- [41] Weglein A B, Tan T H, Shaw S A, Matson K H and Foster D J 2000 Prediction of the wavefield anywhere above an ordinary towed streamer *70th Ann. Int. SEG Mtg (Calgary, Alberta, 2000)*
- [42] Weglein A B 1999 Multiple attenuation: an overview of recent advances and the road ahead *Leading Edge* **18** 40–4
- [43] Berkhout A J, Verschuur D J and Weglein A B 2000 Wave theoretic multiple attenuation: part I *Conf. on Offshore Technology (Houston, TX, 2000)*
- [44] Weglein A B, Matson K H and Berkhout A J 2000 Wave theoretic multiple attenuation: part II *Conf. on Offshore Technology (Houston, TX, 2000)*
- [45] Weglein A B, Foster D J, Matson K H, Shaw S A, Carvalho P M and Corrigan D 2002 Predicting the correct spatial location of reflectors without knowing or determining the precise medium and wave velocity: initial concept, algorithm and analytic and numerical example *J. Seism. Explor.* **10** 367–82
- [46] Shaw S A and Weglein A B 2003 Imaging seismic reflection data at the correct depth without specifying an accurate velocity model: initial numerical examples of an inverse scattering subseries *Frontiers of Remote Sensing Information Processing* ed C H Chen (Singapore: World Scientific)
- [47] Aki K and Richards P G 2002 *Quantitative Seismology* 2nd edn (Mill Valley, CA: University Science Books) p 704
- [48] Sen M and Stoffa P L 1995 *Global Optimization Methods in Geophysical Inversion* (Amsterdam: Elsevier) p 294
- [49] Shaw S A, Weglein A B, Foster D J, Matson K H and Keys R G 2003 Isolation of a leading order depth imaging series and analysis of its convergence properties, in preparation
- [50] Zhang H and Weglein A B 2003 Target identification using the inverse scattering series; inversion of large-contrast, variable velocity and density acoustic media, in preparation

### Further reading

- Amundsen L 2001 Elimination of free-surface related multiples without need of the source wavelet *Geophysics* **66** 327–41
- Carvalho P M, Weglein A B and Stolt R H 1991 Examples of a nonlinear inversion method based on the  $T$  matrix of scattering theory: application on multiple suppression *61st Ann. Int. SEG Mtg* pp 1319–22 (expanded abstracts)
- Carvalho P M, Weglein A B and Stolt R H 1992 Nonlinear inverse scattering for multiple suppression: application to real data: part I *62nd Ann. Int. SEG Mtg* pp 1093–5 (expanded abstracts)
- Devaney A J 1989 Structure determination from intensity measurements in scattering experiments *Phys. Rev. Lett.* **62** 2385–8
- Dragoset W H 1992 Surface multiple attenuation—theory, practical issues, examples *EAGE Abstracts* BO27
- Ikelle L T and Weglein A B 1996 Attenuation of free-surface multiples in multi-offset VSP data *J. Seism. Explor.* **5** 363–78
- Kennett B L N 1979 The suppression of surface multiples on seismic records *Geophys. Prospect.* **27** 484–600
- Manin M and Spitz S 1995 3D attenuation of targeted multiples with a pattern recognition technique *57th EAGE Conf. (Glasgow)* BO46 (expanded abstracts)
- Matson K H, Paschal D and Weglein A B 1999 A comparison of three multiple attenuation methods applied to a hard water-bottom data set *Leading Edge* **18** 120–6
- Matson K and Weglein A B 1996 Free-surface elastic multiple removal using inverse scattering *Canadian SEG* (expanded abstracts)
- Matson K H and Weglein A B 1996 Removal of elastic interface multiples from land and ocean bottom data using inverse scattering *66th Ann. Int. SEG Mtg (Denver, CO, 1996)* pp 1526–9 (expanded abstracts)
- Newton R G 1981 Inversion of reflection data for layered media: a review of exact methods *Geophys. J. R. Astron. Soc.* **65** 191–215
- Riley D C and Claerbout J F 1976 2D multiple reflections *Geophysics* **41** 592–620
- Snieder R 1990 The role of the Born approximation in nonlinear inversion *Inverse Problems* **6** 247–66
- Snieder R 1991 An extension of Backus–Gilbert theory to nonlinear inverse problems *Inverse Problems* **7** 409–33
- Stolt R H and Jacobs B 1981 An approach to the inverse seismic problem *SEP Rep.* **25** 121–32



- 
- Weglein A B 1985 The inverse scattering concept and its seismic application *Developments in Geophysical Exploration Methods* vol 6, ed A A Fitch (Amsterdam: Elsevier) pp 111–38
- Weglein A B 1995 Multiple attenuation: recent advances and the road ahead *65th Ann. Int. SEG Mtg* pp 1492–5 (expanded abstracts)
- Wolf E 1969 Three dimensional structure determination of semi-transparent objects from holographic data *Opt. Commun.* **1** 153